Available online at www.sciencedirect.com

SCIENCE DIRECT®

Journal of Geochemical Exploration 86 (2005) 1–25

JOURNAL OF GEOCHEMICAL EXPLORATION

www.elsevier.com/locate/jgeoexp

Trace element contents in galena and sphalerite from ore deposits of the Alcudia Valley mineral field (Eastern Sierra Morena, Spain)

F.J. Palero-Fernández[a], A. Martín-Izard[b,*]

[a]Servicio de Geología, Minas de Almadén y Arrayanes, S.A., 13400 Almadén, Spain
[b]Departamento de Geología, Universidad de Oviedo, Arias de Velasco s/n, 33005 Oviedo, Spain

Received 8 October 2002; accepted 22 March 2005
Available online 26 May 2005

Abstract

The Alcudia Valley mineral field was an important lead ore producer in Spain during the 19th and the 20th centuries. Based on mineralogical, lithological, structural, morphological and geochemical characteristics, five main types of lead and zinc deposits have been defined in the district. The most important of these are Pb–Zn post-tectonic veins (type E), which represent 70% of the total number of mineral occurrences and include the biggest mines of the area. These deposits show a paragenetic zoning with respect to the Hercynian granites outcropping in the area, with deposits located closer to the granites having a more complex paragenesis than those located farther away and silver showing a decrease away from the granite along three silver corridors [Palero, F.J., Both, R.A., Arribas, A. Boyce, A.J., Mangas, J. and Martín-Izard, A., 2003. Geology and metallogenic evolution of the polymetallic deposits of the Alcudia Valley mineral field, Eastern Sierra Morena, Spain. Economic Geology, 98, 577–605].

Trace element contents in galena concentrates and, particularly, sphalerite concentrates from the Alcudia Valley deposits have allowed us to discriminate between the different ore deposit types. Statistical analysis indicates that trace elements in galena and sphalerite are present mainly as micro-inclusions of various minerals. Sulfides in type E deposits show the widest variety and highest contents in trace elements. The possibility of using trace elements as tools for the characterization of the different types of ore deposits and their regional zoning is the main conclusion reached in this paper. This conclusion may be applied to exploration for these types of ore deposits in other areas with comparable geological characteristics.

Keywords: Galena; Sphalerite; Trace elements; Pb–Zn deposits; Vein type; Iberian Massif

1. Introduction

The Alcudia Valley area is located in the southern central part of the Iberian Peninsula, approximately 250 km south of Madrid. The area was an important Pb–Zn–Ag producer during the late 19th and early

* Corresponding author. Tel.: +34 985103095; fax: +34 985103103.
E-mail address: amizard@geol.uniovi.es (A. Martín-Izard).

0375-6742/$ - see front matter © 2005 Elsevier B.V. All rights reserved.
doi:10.1016/j.gexplo.2005.03.001

20th century and is located within a broad metallogenic province, known as the Sierra Morena, which occupies a part of the Ossa-Morena Zone and the southern limit of the Central Iberian Zone of the Hercynian Belt. This metallogenic province was the major lead producer in Spain during the second half of the 19th century and the Alcudia Valley was one of the most important districts. From the 1930s onwards, production fell and in 1988 the last mine, San Quintin, was closed.

Most of the Sierra Morena Pb–Zn ore deposits are vein type with similar mineral parageneses. However, in the Alcudia Valley the deposits have more heterogeneous mineral assemblages, and five different types can be distinguished, four of them with vein morphology. A total of 484 old mines and prospects are located in an area of approximately 2500 km^2 (Palero et al., 1992), most of them (453) being Pb–Zn veins. Other metals produced in the area were Ag, Cu, Sb, Sn, W, As and Bi. Although many of the deposits were small in size, San Quintín (500,000 Mt of Pb metal), El Horcajo (300,000 Mt of Pb metal), and Diógenes (200,000 Mt of Pb metal) were important producers.

Palero (1991) and Palero et al. (1992) distinguished five types of Pb–Zn deposits based on morphological, mineralogical, paragenetical and geochemical data. Each of the five types was the result of distinct mineralizing processes that acted during different events in its geological history. Palero et al. (2003), mainly using new geochemical data, established the timing of mineralizing processes and redefined the five types from the oldest (A) to the youngest (E). García de Medinabeitia (2003), demonstrated clear differences in lead isotope compositions and different model ages for each type.

Palero (1991) analyzed Ag and Cd content in bulk-ore. The Ag content in type E deposits showed a regional distribution according to the position and distance of the deposits with respect to the Hercynian granite, but Cd contents did not show this relationship (Palero, 1991 and Palero and Martín-Izard, 1992). Also, using the analyses on sphalerites from the Alcudia Valley performed by De Gyves (1988), Palero (1991) found that each deposit type (A–E) shows a different trace element pattern. In view of the interesting results obtained in the previous work we decided to perform a detailed study of trace element contents in sphalerite and galena from the Alcudia Valley, the results and discussion of which are the aim of this paper.

Published papers on the behaviour of trace elements in ores are scarce and only focused on Mississippi Valley deposits (MVT) in the USA (Hall and Heyl, 1968; Viets et al., 1992). There have also been some classification attempts based on the silver content in the ore, such as the works by Bauchau (1971) and Beaudoin and Sangster (1992), but the content of these papers is far from the topic of the present work. Arribas Moreno (1981) tried to characterize Pb–Zn deposits in the Iberian Peninsula based on trace elements, but the enormous scale of the work and the lack of definition of the metallogenic processes led to unclear conclusions.

2. Geological setting

The most important geological feature of the Alcudia Valley region is a series of major Hercynian WNW–ESE trending anticlines and synclines. These structures belong to the southern part of the Central Iberian Zone (Julivert et al., 1972) of the Iberian massif (Fig. 1) and are included in the vertical fold domain defined by Díez Balda et al. (1990). The most extensive anticline structure of this domain is located along the Alcudia Valley itself.

The lithostratigraphic sequence is composed of siliciclastic rocks with some interlayered volcanics and rare carbonate levels. The sequence is made up of four sedimentary cycles bounded by unconformities (Figs. 2 and 3). The first two cycles are Neoproterozoic in age (Riphean–Vendian) and are known as “Alcudiense” (Tamain, 1972). The “Lower Alcudiense” unit is of turbiditic affinity, while the “Upper” one is interpreted as being shelf sediments with syn-sedimentary tectonic activity (Bouyx, 1970; Ortega and González-Lodeiro, 1986; Álvarez Nava et al., 1988; Palero, 1993). Overlying these two units is a Lower Ordovician to Lower Devonian sequence with inter-layered volcanic rocks which was deposited on a stable marine shelf with several sea level oscillations (Tamain, 1967, 1972; García Sansegundo et al., 1987; Palero, 1991, 1992). The fourth sedimentary cycle is made up of a monotonous black shale unit of Visean–Namurian in age known as “Culm de Los Pedroches”,

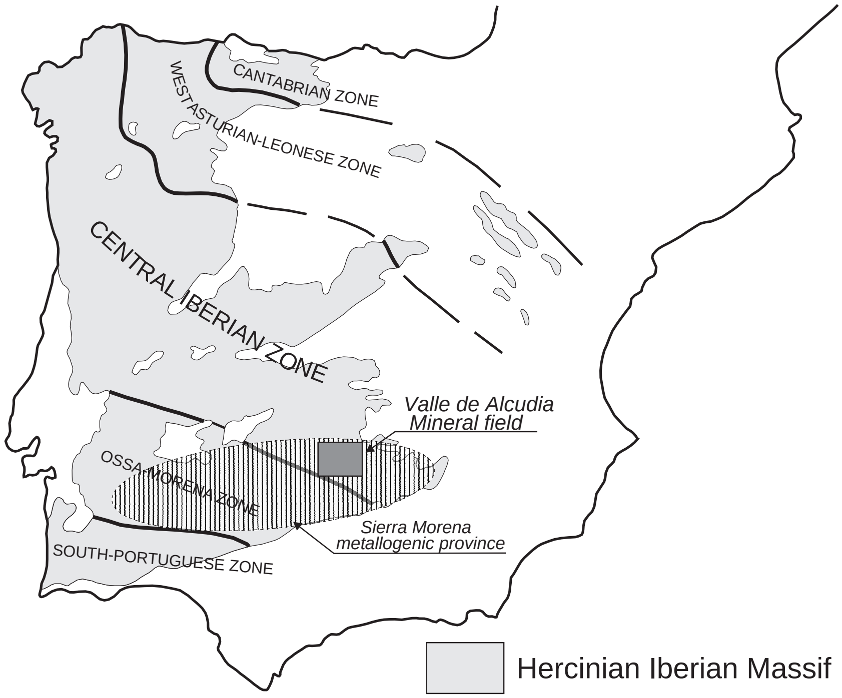

Fig. 1. Location of Alcudia Valley mineral field in the Hercynian Iberian massif.

which was deposited in a rapidly subsiding marine shelf (Peran and Tamain, 1967; Tamain, 1972; Pérez Lorente, 1979; Rodríguez Pevida et al., 1990).

Shortly after deposition of the "Culm", the Hercynian Orogeny took place in the region. The Stephanian B–C coal-rich sediments of the Puertollano Basin (Wagner, 1983) represent the beginning of local post-orogenic sedimentation. The Paleozoic sequence is covered in places by Tertiary detrital continental sediments.

The deformation processes in the region took place during three tectonic events: a pre-Ordovician, a Hercynian and a post-Carboniferous. Two pre-Ordovician episodes are recognized in the area. The first episode folded the Lower Alcudiense rocks as cover folds related to a vertical movement of rigid basement (Ribeiro, 1974). The second episode took place after deposition of the upper Alcudiense sedimentary sequence and involved vertical movements along NW–SE fractures, probably during the Cadomian Orogeny (Ortega et al., 1988; Palero, 1993). As a result of this, the pre-Ordovician geological structures are generally oriented NW–SE due to the important control of basement fractures that were reactivated several times during the Neoproterozic (Ortega et al., 1988).

The Hercynian Orogeny affected both the Neoproterozoic and Paleozoic sedimentary rocks. Two tectonic phases are recognized. The first (F1), Westfalian A–C in age, involved N–S shortening of the crust and generated WNW–ESE synclines and anticlines with reverse and normal faults hosting Zn–Pb–Cu mineralization along the fold axes (Fig. 2). The second Hercynian phase (F2), Stephanian B in age, involved E–W shortening that generated conjugate sinistral NW–SE and dextral ENE–WSW brittle–ductile shear zones (Fig. 2) (Roiz, 1979; Ortega, 1988; Wallis, 1985). The best developed shear zones are sinistral NW–SE and appear to be related to reactivation of basement fractures with the same orientation. Fracturing related to shearing is very important from a metallogenic point of view, as most of the mineral deposits in this study are hosted in fractures that developed during this tectonic event. The regional Hercynian metamorphic grade is sub-greenschist facies (Tamain, 1972; Saupe, 1973; Leal Echevarría et al., 1976), with minor recrystallization and soft slaty-cleavage.

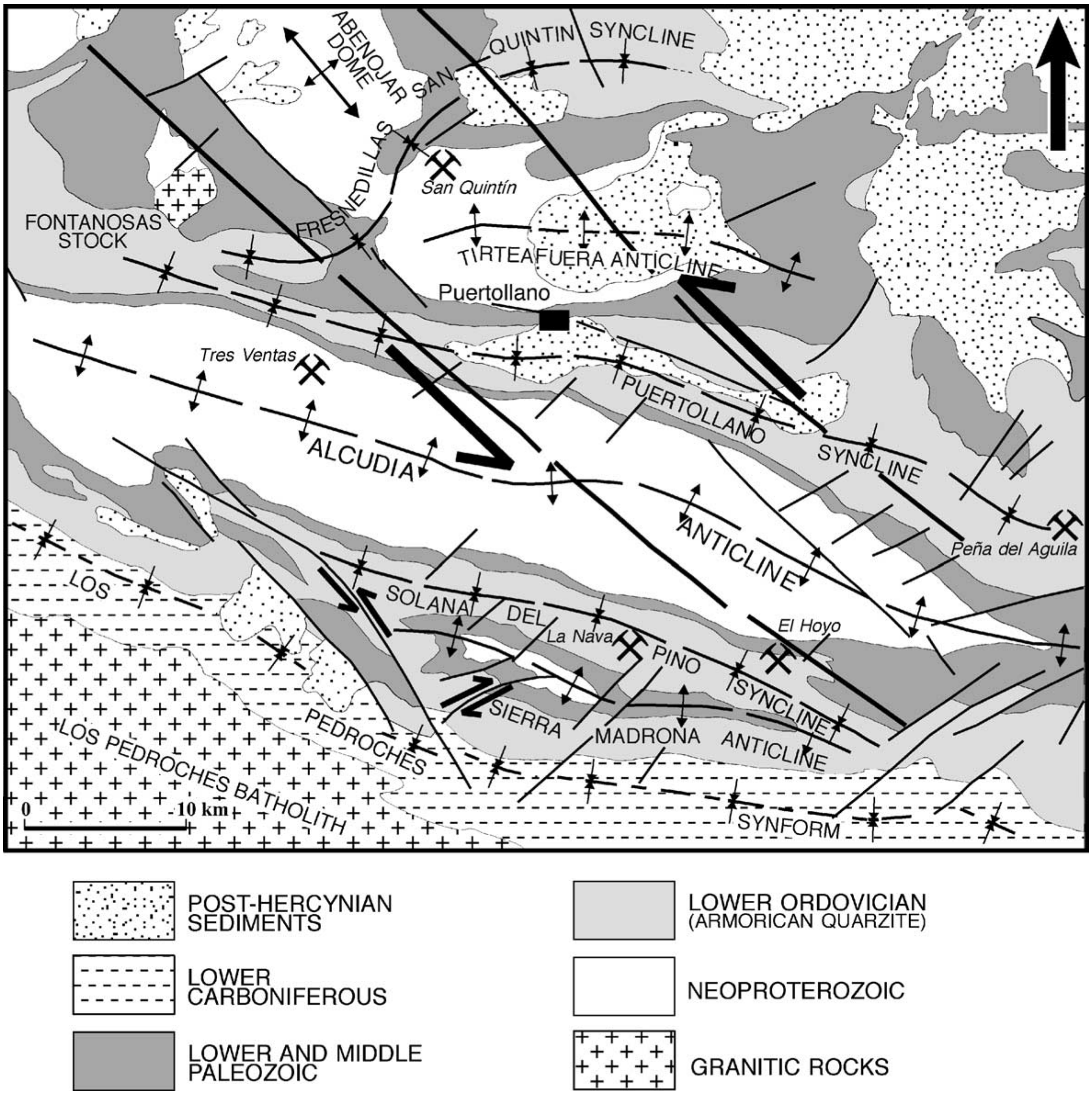

Fig. 2. Geological sketch of the Alcudia Valley region with major structural features of the mineral field and location of the deposit model of each type. (Type A: Peña del Aguila, type B: El Hoyo, type C: La Nava, type D: Tres Ventas, type E: San Quintín).

The post-Carboniferous deformations are of minor importance in the Alcudia Valley region, and generated N–S, NE–SW and NW–SE trending faults. It is difficult to precisely define the age of these movements but they post-date all five types of mineral deposits. In our opinion the latest movements could be Alpine.

Magmatic activity took place in three episodes. The first was Paleozoic syn-sedimentary volcanism of variable composition (García Sansegundo et al., 1987; Palero and Martín-Izard, 1988; Palero, 1991, 1992; Higueras and Acosta, 1992). The second was granite intrusion related to the Hercynian orogeny. Finally, there was the Pliocene–Pleistocene volcanic activity known as Campos de Calatrava basalts (Gallardo et al., 1998; Ancoechea, 1983).

Hercynian granite magmatism is Carboniferous in age (305–291 Ma, Penha and Arribas, 1974; 302 Ma,

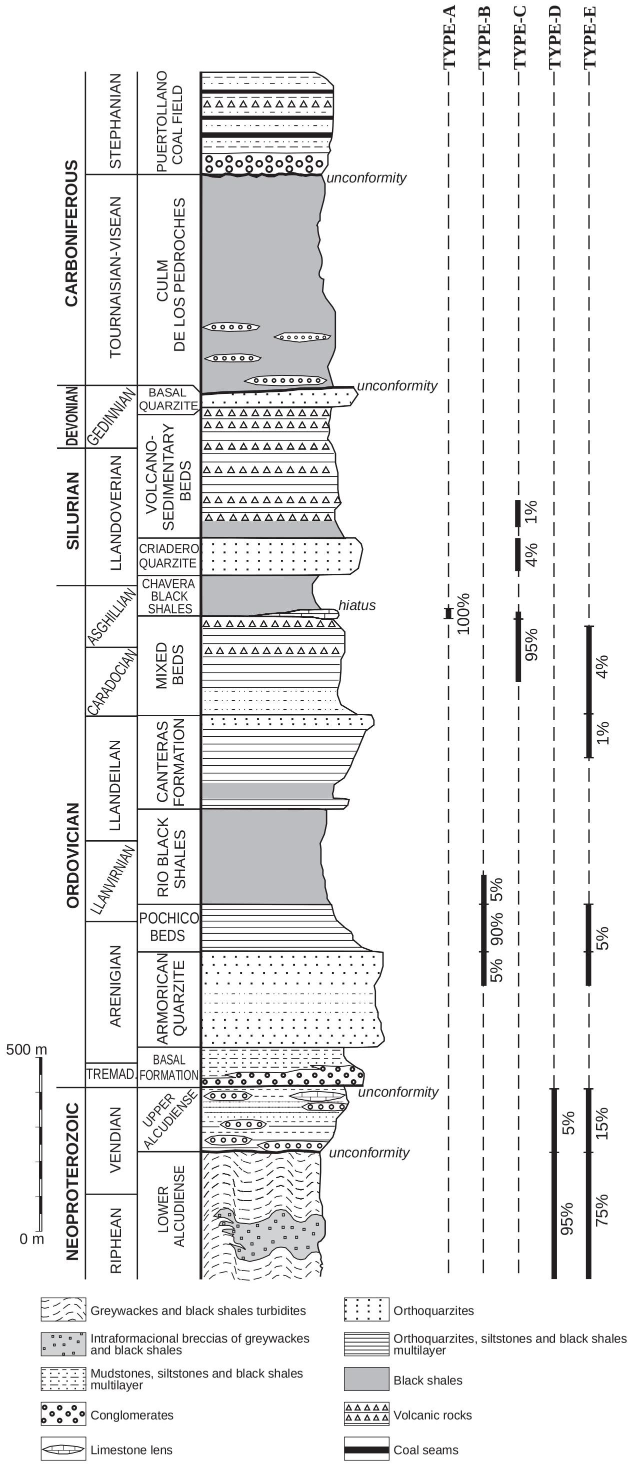

Fig. 3. Lithostratigraphic column of Neoproterozoic and Paleozoic sequences in the Alcudia Valley mineral field and distribution of mineral deposit types (After Palero, 1992 and Palero et al., 2003).

Leutwein et al., 1970; 320–299 Ma, Defalque et al., 1992; 309 Ma, Larrea et al., 1999; 329–293 Ma, García de Medinabeitia, 2003) and formed large intrusive S-type granitoids, which developed wide contact metamorphic aureoles. In the Alcudia Valley two intrusions are present, the Fontanosas pluton and Los Pedroches batholith. The former (Fig. 2) is a small rounded equigranular granodiorite surrounded by Neoproterozoic rocks (Saupe, 1973; García Sansegundo et al., 1987; Amor and Ortega, 1987). The latter (Fig. 2) is a large WNW–ESE elongate granite batholith in which two facies, equigranular granodiorite and porphyritic monzogranite, can be recognized (Leal Echevarría et al., 1976; Donaire and Pascual, 1992). The monzogranite is intrusive in the granodiorite. The granodiorite emplacement took place after the first Hercynian tectonic event and prior to, or simultaneously with, the second (Coupez et al., 1988), and monzogranite emplacement took place after the second Hercynian tectonic event. Several small W, Sn, As and Bi deposits are apparently related to these igneous rocks.

3. Lead and zinc deposit types in the Alcudia Valley mineral field

The Alcudia Valley Pb–Zn deposits were classified by Palero (1991) and Palero et al. (1992) into five types, based on their morphology, host rock relations, structural setting, mineral assemblages and geochemical data (Table 1). Using new geochemical data, Palero et al. (2003) were able to obtain a better knowledge of the metallogenetic processes involved in the formation and chronology of the five types. The following groups were established (Palero et al., 2003) in relation to the Hercynian Orogeny: pretectonic deposits (type A), syntectonic deposits (types B, C and D) and post-tectonic deposits (type E).

The main characteristics of the different types are summarized in Table 1 and discussed below. Of the five deposit types the most important, from an economic point of view and with regard to the number of occurrences, is type E. This type of mineralization represents 70% of the total number of mines and prospects and also includes the biggest mines of the area. Type A is scarce, with only 2% of the deposits. Type D represents 6%, type B 12% and type C 5%. The remaining 5% correspond to Sn, W, As, Bi, Cu and Sb deposits not included in this classification.

Type A deposits are Zn–Pb stratabound ores that found as disseminations or micro-veins in the top of the Urbana Limestone, the only carbonate unit in the Paleozoic sequence (Fig. 3). Mineralization consists of sphalerite with lesser amounts of galena, quartz and dolomite and was contemporaneous with silicification, followed by dolomitization (Castroviejo, 1979; Palero and Martín-Izard, 1988). Type A deposits (Palero and Martín-Izard, 1988; Palero et al., 2003) probably formed by diagenetic metasomatism of the overlying Chavera Black Shales which are geochemically anomalous in Mg–Zn–Pb–S, among other elements.

Type B deposits are Zn–Pb–Cu veins in highly deformed WNW–ESE breccias in siliceous layers of the Pochico Beds (Fig. 3), which are related to reverse and, occasionally, normal faults generated during the first Hercynian phase (F1). The mineral association consists of pyrite, sphalerite, galena, chalcopyrite and quartz that is associated with strong silicification and minor chloritization of the host rock. The sequence of deposition was pyrite followed by galena, sphalerite and chalcopyrite, and later quartz. Isotope compositions of sulfur ($\delta^{34}S$) in the sulfides (Table 1) are similar to diagenetic pyrite in the Pochico (Palero et al., 2003). Type B deposits involve lateral secretion–migration of fluids and metals from the Pochico Beds into the fault-bearing open spaces and breccia faults. This process took place during synkinematic conditions at the end of the first Hercynian phase and during the subsequent extension when compression ended (Palero, 1986; Delgado et al., 1988; Palero et al., 2003).

Type C deposits are Zn–Pb veins and stockworks in fractures and breccias mainly related to brittle F2 Hercynian shear zones that affected the upper part of the Mixed Beds (Fig. 3). Mineralization consists of sphalerite with minor galena, quartz and carbonate and the host rock is partially silicified, carbonatized and chloritized. Siderite and ankerite were the first minerals to be deposited, followed by quartz and sulfides. The isotopic composition of sulfur in the sulfides is similar to type A deposits (Table 1). Type C deposits were formed by migration of fluids and elements from the black shales, mainly the Chavera

Table 1
Summary of characteristics of the Alcudia Valley mineral deposit types

Type of deposit	Paragenetic association[a]	Host rock	Morphology	Host rock alteration	Mineralization			Sulphur isotopes[b]	Lead isotopes[c]	Probable formation age[d]
					Ore	Gangue	Textures			
Type A	Sp–Gn–Qtz–C	Upper Ordovician "Urbana Limestone"	Stratabound	Strong silicification and dolomitization	**Sphalerite**, **galena**, (chalcopyrite), (pyrite)	**Quartz**, **dolomite**	Granular	Gn = 8.3‰ Sp = 10.7 to 3.6‰		Lower Paleozoic (Silurian)
Type B	Py–Sp–Gn–Ccp–Qtz	Lower Ordovician "Pochico Beds"	Milonitic and breccia veins	Strong silicification weak chloritization	**Pyrite**, **sphalerite**, **galena**, chalcopyrite, (pyrrhotite), (bournonite), (tetrahedrite), (marcasite)	**Quartz**, (chlorite), (siderite)	Milonitic and tectonic breccias	Gn = −0.7 to 12.6‰ Sp = 4.2 to 17.0‰ Py = 7.4 to 8.4‰	$^{206}Pb/^{204}Pb = 18.039 \pm 0.034$ $^{207}Pb/^{204}Pb = 15.654 \pm 0.017$ $^{208}Pb/^{204}Pb = 38.253 \pm 0.058$ model age = 545 ± 10 Ma	Westphalian
Type C	Sp–Gn–Qtz–Ank	Upper Ordovician"Mixed Beds"	Breccia stockworks and milonitic veins	Weak silicification chloritization carbonatization	**Sphalerite**, **galena**, (chalcopyrite), (pyrite), (bournonite), (tetrahedrite), (linneite)	**Quartz**, ankerite, (siderite), (calcite)	Milonitic, tectonic breccias, banded and cockade	Gn = 7.3 to 11.0‰ Sp = 10.7 to 13.3‰	$^{206}Pb/^{204}Pb = 18.047 \pm 0.033$ $^{207}Pb/^{204}Pb = 15.677 \pm 0.012$ $^{208}Pb/^{204}Pb = 38.220 \pm 0.043$ model age = 583 ± 14 Ma	Westphalian–Stephanian
Type D	Sp–Gn–Qtz–(Ank)	Neoproterozoic	Milonitic veins	Weak silicification chloritization sericitization	**Sphalerite**, **galena**, chalcopyrite, (pyrite), (bournonite), (tetrahedrite), (ullmannite)	**Quartz**, siderite, ankerite, (moscovite), (chlorite)	Milonitic, granular and tectonic breccias	Gn = −8.6 to 4.7‰ Sp = −12.7 to 3.1‰	$^{206}Pb/^{204}Pb = 17.764 \pm 0.016$ $^{207}Pb/^{204}Pb = 15.576 \pm 0.009$ $^{208}Pb/^{204}Pb = 37.745 \pm 0.039$ model age = 600 ± 13 Ma	Stephanian
Type E	Gn-(Sp)-(Ccp)-Ank	Neoproterozoic and lower Paleozoic multilayer units	Breccia veins	Weak chloritization carbonatization silicification sericitization	**Galena**, sphalerite, chalcopyrite, pyrite, marcasite, (arsenopyrite), (bournonite), (boulangerite), (pyrrhotite), (proustite), (freibergite), (tetrahedrite), (linneite), (millerite), (ullmannite), (stibnite)	**Ankerite**, barite, quartz, calcite, (chlorite)	Tectonic breccias, cockade, banded and vugs	Gn = −9.8 to −2.7‰ Sp = −6.0 to −3.4‰ Py = −23 to −5.5‰	$^{206}Pb/^{204}Pb = 18.188 \pm 0.030$ $^{207}Pb/^{204}Pb = 15.614 \pm 0.014$ $^{208}Pb/^{204}Pb = 38.300 \pm 0.061$ model age = 356 ± 21 Ma	Permian–lower Triasic

Minerals in bold are the most abundant and those in brackets are scarce and sporadic.

[a] Mineral symbols after Kretz (1983).

[b] $\delta^{34}S$ data after Palero et al. (2003).

[c] Data after García de Medinabeitia (2003).

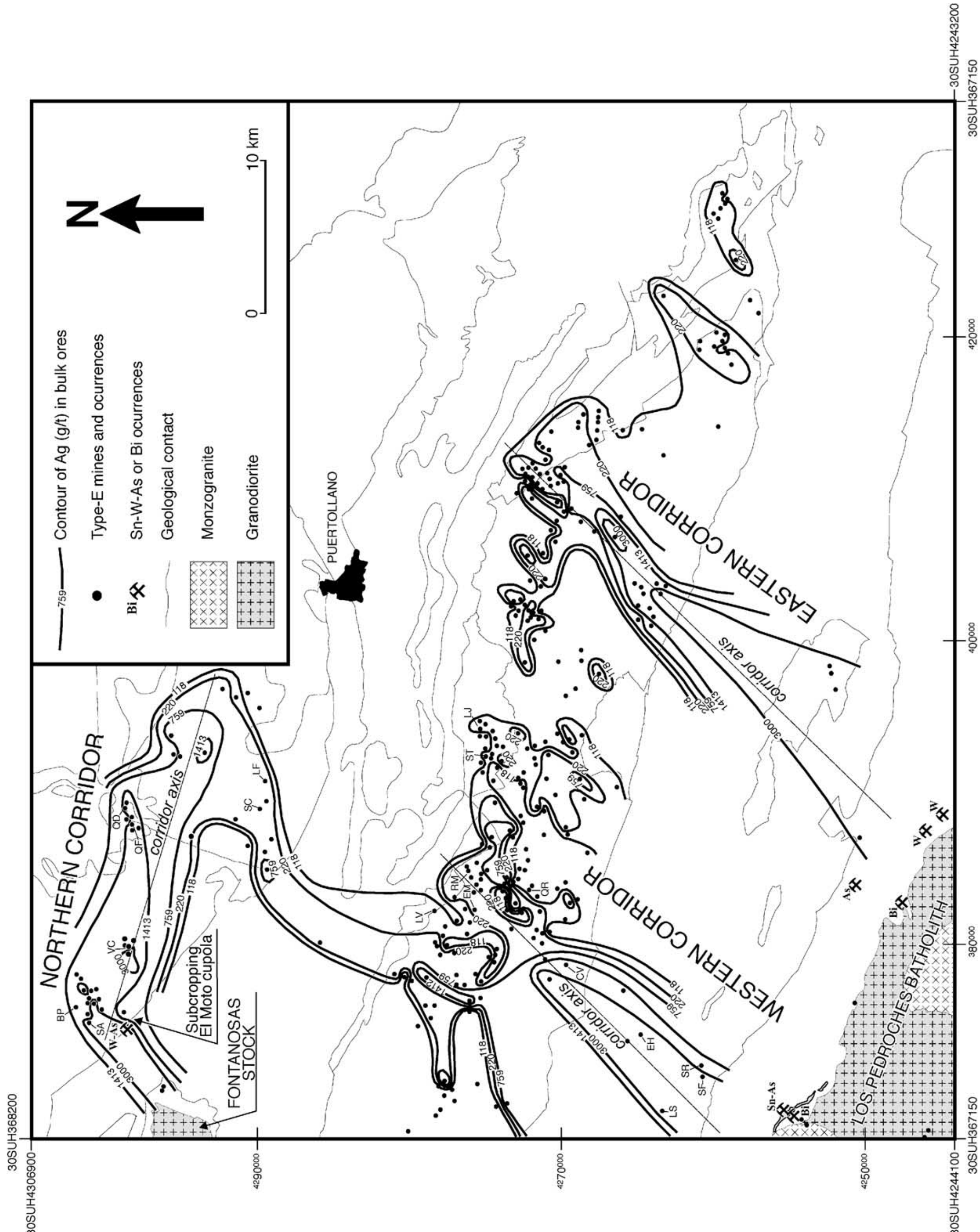
Contour of Ag (g/t) in bulk ores
Type-E mines and ocurrences
Sn-W-As or Bi ocurrences
Geological contact
Monzogranite
Granodiorite
N
0
10 km
PUERTOLLANO
NORTHERN CORRIDOR
WESTERN CORRIDOR
EASTERN CORRIDOR
corridor axis
Subcropping El Moto cupola
FONTANOSAS STOCK
LOS PEDROCHES BATHOLITH
30SUH368200
30SUH4306900
30SUH367150
30SUH4243200
30SUH4244100

Black Shales and to a lesser degree the Volcano-sedimentary Beds, into faults and breccias that developed during Hercynian F1 folding and F2 shearing phases. The minerals show evidence of synkinematic formation conditions, but the intensity of deformation varies from place to place (Palero, 1991; Palero et al., 2003).

Type D deposits are Zn–Pb deposits hosted in strike-slip faults trending WNW–ESE (most important), NW–SE and ESE–WSW. These fractures are related to Hercynian F2 shear zones affecting Neoproterozoic rocks. Mineralization consists of a first stage of sphalerite (the most abundant sulfide), galena and quartz, which are highly deformed, and a second stage consisting of undeformed pyrite and ankerite in host rock that is incompletely silicified, sericitized and chloritized. They are synkinematic and show a close relationship with F2 Hercynian shear zones (Palero et al., 2003).

Type E is the main group of deposits in the Alcudia Valley. These are Pb, Pb–Zn and Pb–Ag veins with breccia textures in NE–SW, E–W and NW–SE tensional fractures that developed during the F2 Hercynian shortening, mainly in Neoproterozoic rocks. Alteration of the host rocks is weak, consisting of carbonatization and chloritization with minor silicification and sericitization. Five stages of hydrothermal mineral deposition can be defined, but not all stages are present in all deposits. The stages are represented by the following minerals:

Early: arsenopyrite, pyrrhotite and microcrystalline quartz.
Ag-rich: sulfosalts (bournonite, freibergite).
Main: abundant galena and ankerite. This stage is present in all deposits and characterizes type E.
Late: sphalerite and quartz.
Final: barite, pyrite and calcite.

The first three stages show continuity in their crystallization and fill open spaces. After their formation, further brecciation developed and the late stage mineralization cemented the newly formed breccias. The final stage filled the last open spaces in the breccias.

The ore mineral assemblages are more complex and more Ag-rich close to the igneous bodies (Palero, 1991). In deposits located close to the intrusive bodies, the first three stages are present. Farther away from the granitoids, only the Ag-rich and main stages can be found. The silver minerals disappear progressively outward from the granitoids and zones located farther from granites contain only galena and ankerite.

The silver content in the bulk ores also reflects this zoning and defines the so-called “silver corridors” (Fig. 4). Near the igneous intrusions, in these “silver corridors” there are also W–Sn–As and Bi deposits, and the silver content of the corridors decreases outward from the granites. The decrease occurs not only along the corridor but also laterally outward from the axis of each corridor (Palero and Martín-Izard, 1992; Palero et al., 2003).

The paragenetic zoning described and the deposit distribution within the “silver corridors” suggests that the type E deposits are related to the Hercynian granitoids (Palero, 1991). The granitoids could well have acted as a thermal focus causing hydrothermal convective circulation, in which the heat necessary to generate the hydrothermal fluid was provided by the granites, according to the model proposed by Simpson et al. (1979) and Plant et al. (1983). The corridors could indicate the paths followed by the hydrothermal fluid away from the granites through the metasedimentary rocks.

The S isotope composition of galena (Table 1) and also C and O isotope composition of ankerite (− 10.80 to − 16.00, and 17.20 to 23.10 respectively) suggest that the metasedimentary host rocks, particularly the Neoproterozoic materials, were the main source components in the type E deposits (Palero et al., 2003). However, the Pb isotope composition indicates that lead was extracted from, and recycled by, the granitoids (García de Medinabeitia, 2003), which

Fig. 4. Regional distribution of silver content in bulk ores of type E deposits of the Alcudia Valley mineral field (after Palero and Martín-Izard, 1992 and Palero et al., 2003) and location of deposits mentioned in Figs. 9 and 10 (SA—San Alberto, BP—Buenpensamiento; VC—La Victoria; QF—San Quintín (San Froilán); QD—San Quintín (Don Raimundo); SC—El Campillo; LF—La Fortuna; SF—San Serafín; SR—Santa Rosa; LS—La Salvadora; EH—El Horcajo; CV—Cerro Verde; QR—Quinto del Río; EM—La Emperatriz; RM—La Romanilla; LV—La Veredilla; ST—Santa Teodora; LJ—La Jarosa). The dotted lines are the axes of each corridor calculated as regression lines from the UTM coordinates of each deposit. Contours of silver content have been calculated using frequency distribution analyses.

Table 2
Analytical data of sphalerite concentrates from the Alcudia Valley mineral field deposits

Mine or occurrence	Major elements			Trace elements 1st category					Trace elements 2nd category					
	Zn (%)	S (%)	Fe (%)	Cu (ppm)	Cd (ppm)	Ag (ppm)	Sb (ppm)	Co (ppm)	Mn (ppm)	Ge (ppm)	Ga (ppm)	In (ppm)	As (ppm)	Sn (ppm)
Type B deposits														
La Prometida	54.05	31.05	6.00	14,434	1233	35	1	303	40	5	90	90	<2	72
Eufrasia	62.40	32.26	2.21	870	2680	78	328	381	<7	74	98	283	<2	68
San Bartolomé	59.76	32.13	3.90	2651	1088	13	17	561	35	3	18	11	<2	11
Los Diegos	55.93	30.65	6.08	1925	798	12	83	475	182	3	15	18	<2	<2
Atilana	57.56	31.13	3.44	6991	883	32	80	616	74	<1	32	53	86	<2
Los Diegos	62.09	30.72	0.91	49	1119	6	24	338	35	11	23	<0.5	158	10
Mean	58.63	31.32	3.76	4487	1300	29	89	446	73	19	46	91	122	40
Standard deviation	3.37	0.70	2.05	5439	695	27	122	126	63	31	38	112	51	34
Type C deposits														
Virgen del Socorro	61.88	30.56	1.83	76	477	34	24	484	<7	17	<4	5	13	21
Navalahiguera	65.11	32.93	1.12	428	640	24	55	347	<7	97	4	<0.5	14	<2
Santa Rita	64.33	31.16	1.26	269	618	1	17	259	<7	61	<4	5	19	15
Navalajeta	62.98	30.72	0.98	974	893	44	190	409	<7	58	22	<0.5	13	12
La Nava	65.07	32.98	1.38	964	795	33	68	390	<7	86	<4	<0.5	37	<2
El Contadero	59.61	32.33	4.96	652	984	27	43	276	44	2	<4	<0.5	<2	<2
Mean	63.16	31.78	1.92	561	735	27	66	361	44	54	13	5	19	16
Standard deviation	2.15	1.10	1.52	369	190	15	64	85	0	37	13	0	10	5
Type D deposits														
Tres Ventas	61.37	32.00	2.51	318	2826	23	266	100	<7	38	33	<0.5	69	9
Navalcaballejo	60.37	29.72	2.29	464	2503	25	83	154	53	<1	<4	11	<2	<2
Precaucion	59.24	31.79	5.19	275	1846	15	20	155	97	25	<4	6	2	7
Pepita	63.88	30.90	1.34	134	2538	11	29	172	<7	<1	<4	<0.5	<2	<2
Nacedero	57.28	30.04	4.71	163	1855	1	17	168	38	<1	<4	<0.5	<2	<2
Abundancia	63.95	32.51	1.76	348	1925	20	38	171	<7	23	<4	18	<2	<2
Las Simonas	58.40	30.18	3.48	303	1574	12	15	199	195	49	<4	7	166	<2
San Pantaleón	59.74	29.40	3.56	1517	2483	38	129	566	311	35	<4	66	<2	47
Arroyo del Royar	64.23	32.72	1.37	316	3544	18	25	316	13	<1	<4	5	<2	29
Fajano	61.08	30.60	2.34	322	2632	2	33	163	114	14	<4	52	14	30
Mean	60.95	30.99	2.86	416	2373	17	66	216	117	31	33	24	63	24
Standard deviation	2.43	1.19	1.34	398	585	11	79	135	104	12	0	25	75	17
Type E deposits														
La Boticaria	59.97	32.27	3.74	182	2789	13	4	155	48	35	<4	<0.5	<2	10
Cora Pearl	57.90	31.68	6.07	504	6906	1336	1164	154	36	48	<4	<0.5	<2	17
Villazaide	56.32	32.32	6.80	1211	2572	190	869	273	<7	105	70	12	<2	3
La Veredilla	64.24	32.89	1.36	2224	5135	564	1416	103	<7	<1	<4	50	<2	15
Santa Bárbara	58.33	31.80	4.74	1899	3919	265	1190	224	<7	100	72	27	<2	17
Quinto del Río	61.16	31.96	1.47	2778	4108	452	1690	95	32	28	174	70	162	62
La Petaca	62.26	31.13	1.32	1597	3515	314	1198	137	<7	32	135	73	<2	20
San José	60.24	32.11	3.91	1504	3192	428	1066	152	<7	130	18	<0.5	<2	25
San Quintín (Don Raimundo)	53.06	32.02	7.58	835	2998	347	913	328	<7	105	44	<0.5	201	2
La Romanilla	63.92	32.86	1.44	1664	3682	245	801	122	<7	51	168	140	<2	54
La Boticaria	61.32	32.10	2.83	2256	3057	196	933	225	10	80	233	119	<2	66
La Gitana	59.81	31.95	2.80	3152	2933	306	1310	317	<7	70	234	45	79	27
Paraje Encinarejo	60.99	32.49	3.44	2532	4454	386	1511	212	<7	77	64	138	<2	47

Table 2 (*continued*)

Mine or occurrence	Major elements			Trace elements 1st category					Trace elements 2nd category					
	Zn (%)	S (%)	Fe (%)	Cu (ppm)	Cd (ppm)	Ag (ppm)	Sb (ppm)	Co (ppm)	Mn (ppm)	Ge (ppm)	Ga (ppm)	In (ppm)	As (ppm)	Sn (ppm)
Santa Bárbara	58.46	31.85	5.43	1245	3700	180	846	283	<7	100	<4	7	<2	<2
San Quintín (San Froilán)	52.99	31.28	8.25	908	2907	658	1210	167	<7	42	18	18	284	38
Mean	59.40	32.05	4.08	1633	3724	392	1075	196	32	72	112	64	182	29
Standard deviation	3.36	0.49	2.33	850	1122	307	393	76	16	33	81	49	85	21

Samples were analyzed by X-ray fluorescence at the Autonoma University of Barcelona (De Gyves, 1988).

must have been the source of lead and other metals in the hydrothermal system. This is in agreement with the paragenetic zoning previously described and the presence in the "silver corridors" of several occurrences of W–Sn–As and Bi mineralization that might be directly related to the granitoids (Neiva, 1982; Rundquist, 1982; and Arribas Moreno et al., 1988).

The late and final stages of mineralization, as pointed out by Palero et al. (2003), are related to the late-Hercynian movements and do not show any genetic relationship to the granites.

4. Geochemistry of ore minerals

4.1. Sampling, sample preparation and analysis

To characterize the five deposit types geochemically, about 400 samples of approximately 5 kg each of lead and/or zinc ores were collected. Where possible, samples were taken in situ from ore bodies. In other cases, the mineralized samples were taken from dumps. In each orebody or dump, several samples were taken from different places in order to obtain representative material for the whole deposit.

The samples were crushed, homogenized and divided into two parts. The first part was used for bulk ore chemical analysis. The regional distribution of silver ("silver corridors" of Fig. 4) previously mentioned, was established using the bulk ore silver analyses (Palero and Martín-Izard, 1992; Palero et al., 2003).

The second part of each sample was used to prepare high purity concentrates of galena and sphalerite. The samples were crushed again and sieved into five fractions: >1.19, 1.19–0.71, 0.71–0.40, 0.40–0.30, and <0.30 mm. Particles over 1.19 mm and less than 0.30 mm were rejected. Using a binocular microscope the size fraction was selected in which the galena or sphalerite was released. The most frequent fraction used was 1.19–0.71 mm, but in some cases, especially in types A, B and D deposits, 0.71–0.40 and 0.40–0.30 mm fractions were used.

Galena and sphalerite were concentrated by elutriation, a very useful method due to the high differences in density between them and the gangue. Some problems were experienced in separating chalcopyrite and sphalerite where they occurred together. A concentrate of both minerals was first obtained and this was then elutriated again to achieve separation. Galena and sphalerite concentrates were examined and refined by handpicking under a binocular microscope to obtain 10 g of high purity concentrate. Finally the concentrates were powdered in an agate mortar.

The sphalerite concentrates were analyzed for Zn, S, Fe, Cu, Cd, Ag, Sb, Co, Mn, Ge, Ga, In, As and Sn by X-ray fluorescence at the Autonoma University of Barcelona according to the analytical method of De Gyves (1988). Trace element data from sphalerite concentrates were considered valid if the Pb content was below 0.5%, and if the sum of elements (major and trace) was over 92% when the gangue was quartz, or 96% when the gangue was carbonate. With this grade of purity contamination from minerals other than sphalerite is minimal. The total number of valid analyses was 37; all type A and some type E data were not of sufficiently high quality and were excluded.

The galena concentrates were analyzed for Pb, Zn, Sb, Ag, Cu, Mn, Ni, Cd, Sr, Co, Bi, Hg, As, Au, Se, K, Ca, Na, P, Mg and Al by ICP/MS; and S by LECO at Actlabs (Canada). Nevertheless, due to the very high lead content of the samples, a special attack of the samples and equilibration of equipment was necessary. For quality control some samples were analyzed in duplicate and negligible analytical error was detected. Elements such as Ca, Na, P, Mg, Al and K were taken in account as an indication of purity and were only encountered in very low levels, indicative of the high purity of the galena concentrates. Also Zn and Fe were also used as a control of the purity of galena. All samples with a Zn content over 1% were rejected, because the galena could be contaminated by trace elements from sphalerite. Some samples from type E deposits showing Fe contents over 1.5% have been rejected, because iron could indicate some level of ore oxidation. A total of 58 analyses were considered useful for this study, of which 38 are from type E deposits. No valid analyses were obtained of galena concentrates from type A deposits.

4.2. Trace elements in sphalerite concentrates

The analytical results of sphalerite concentrates fall into three groups: major elements (S, Zn, Fe), trace elements referred to as "first category" which are in most cases above the detection limit (Cu, Cd, Ag, Sb, Co), and trace elements referred to as "second category", which are rarely present above the detection limit (Mn, Ge, Ga, In, As, Sn). The data, the mean and standard deviation are shown in Table 2.

From a statistical point of view, the correlation matrix provides information on the occurrence of the elements in sphalerite (Table 3). The correlation analysis is global for all samples (including types B, C, D and E), because comparison of deposit types is not possible because of a lack of adequate data for some types.

The high negative correlation (−0.92344) between Zn and Fe indicates the replacement of Zn by Fe in the sphalerite framework (Table 3). The close correlation between pairs of elements such as Cd–Ag, Cd–Sb, Ag–Sb and In–Sn, with correlation indices (R^2) above 0.75, and the lack of correlation with the major elements (S, Zn, Fe), could indicate submicroscopic inclusions or exolutions of sulfantimonides of Ag and Cd. Also significant is the low correlation between S and Zn, the major elements of sphalerite, indicating that the compositional variations in sphalerite are independent of their S and Zn contents. The high correlation index (R^2=0.76) between In and Sn is more difficult to explain, as are those between Ga–Sn, Ga–In, and Ga–Sb, all of which are over 0.5, especially considering the low correlation indices between these elements and the major elements.

Considering each deposit type, sphalerite concentrates from type B are rich in Cu and Co and poor in Cd, Ag and Sb; those from type C are characterized by relatively low contents in trace elements; those from type-D deposits are rich in Co, Cd and Mn and poor in Cu, Ag and Sb; and those from type E are very rich in Cd, Ag and Sb, poor in Mn and erratic in their As contents, which are sometimes very high.

Pairs of elements with statistical correlations are shown graphically in Fig. 5. In all graphs the samples cluster according to deposit type. Outstanding among

Table 3
Correlation matrix between trace elements in sphalerite concentrates from the Alcudia Valley mineral field

	Zn	S	Fe	Cu	Cd	Ag	Sb	Co	Mn	Ge	Ga	In	As	Sn
Zn	1.00000													
S	.30491	1.00000												
Fe	−.92344	−.07466	1.00000											
Cu	−.36893	−.02309	.21315	1.00000										
Cd	−.05143	.28208	.14048	−.08855	1.00000									
Ag	−.23986	.22439	.32902	−.00587	.78820	1.00000								
Sb	−.15930	.34581	.18816	.06089	.75423	.75923	1.00000							
Co	−.10214	−.20063	.03419	.23100	−.56142	−.35818	−.40172	1.00000						
Mn	−.24730	−.58686	.16227	.02728	−.18466	−.22468	−.34399	.32170	1.00000					
Ge	−.04580	.38989	.18167	−.14447	.20172	.25242	.44665	−.06668	−.30251	1.00000				
Ga	−.00527	.23380	−.10452	.31892	.26216	.18245	.55407	−.14213	−.24630	.25094	1.00000			
In	.09614	.14966	−.14295	.29148	.22562	.05455	.26488	.04192	−.02911	.10517	.54364	1.00000		
As	−.40518	−.12025	.25450	−.03507	−.03231	.20763	.22519	−.04590	.01782	.05535	.08305	−.13662	1.00000	
Sn	−.00281	.08670	−.06823	.43353	.29939	.20690	.35997	−.07675	−.00604	.07420	.62279	.76035	.01042	1.00000

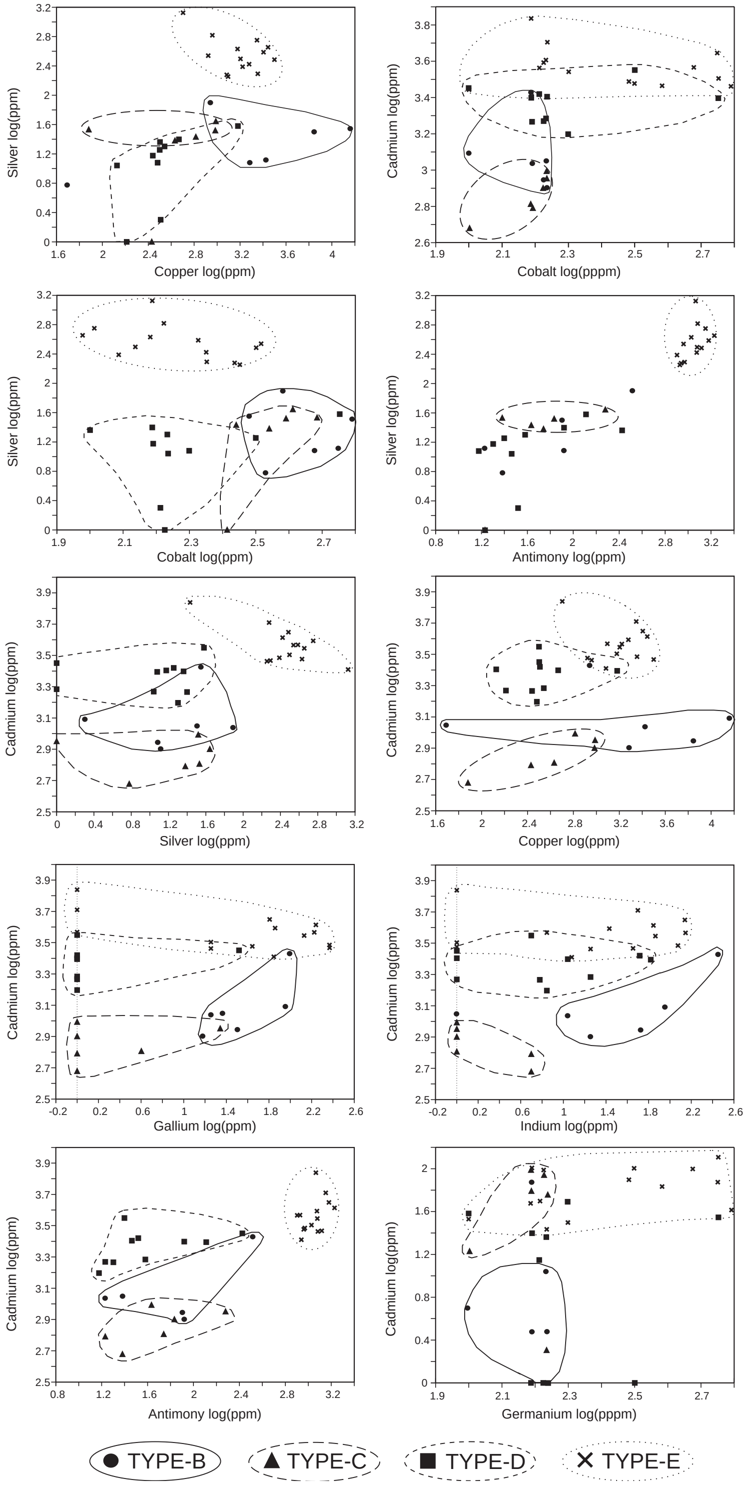

Fig. 5. Scatter plots between pairs of trace elements from Alcudia Valley sphalerite concentrates.

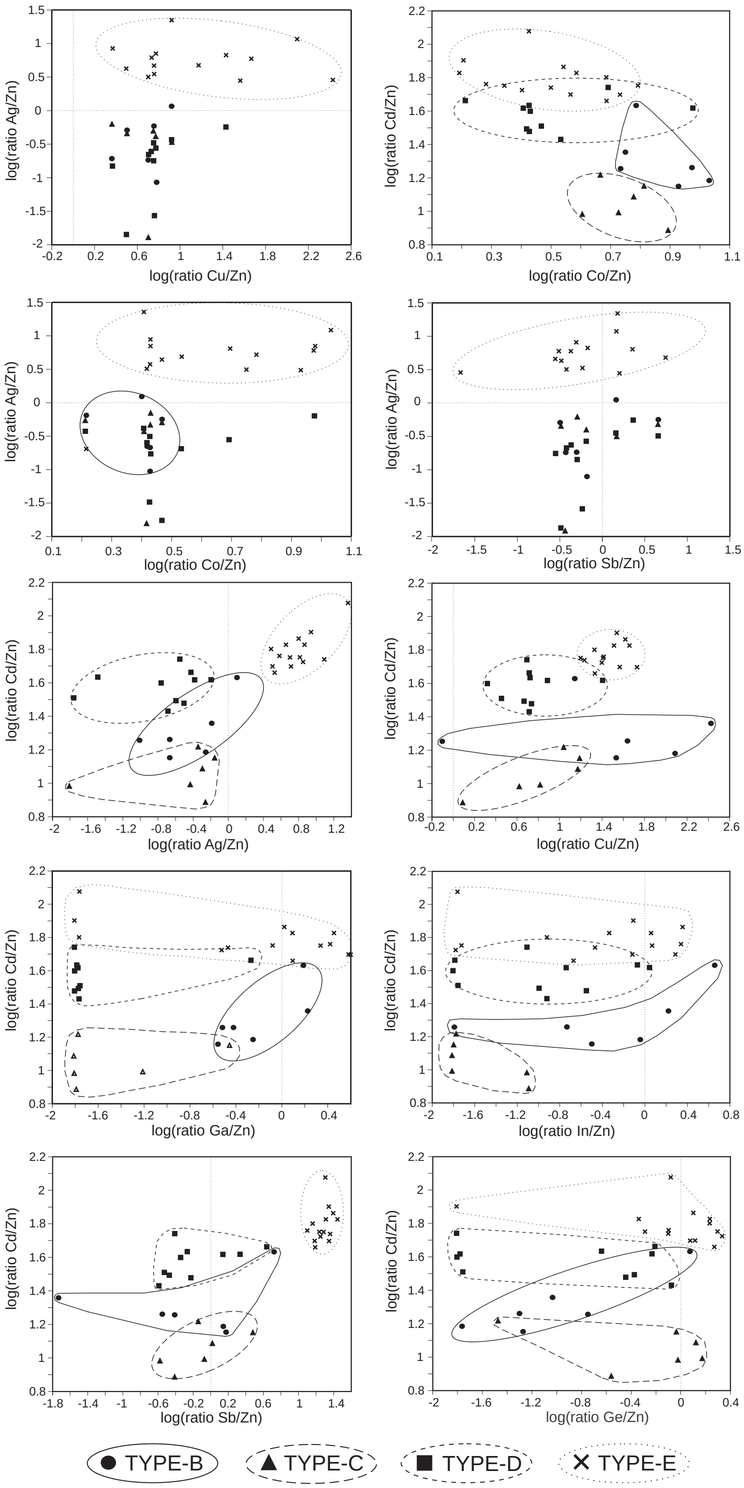

Fig. 6. Scatter plots between pairs of trace elements/Zn ratios from Alcudia Valley sphalerite concentrates.

them is type E, which shows the highest content in the plotted trace elements. In Fig. 6 the same elements are referred to the zinc content of each sample, thus defining more closely fields for each type of deposit. The established correlations for elements such as Cd, Sb, Ag, Cu and Co allow us to discriminate between each type of deposit. The fact that sphalerites from different deposit types have a different content in trace elements could be interpreted as the consequence of different genetic processes for each type.

4.3. Trace elements in galena concentrates

Data of trace elements in galena concentrates have been grouped following the same criteria as for sphalerite into major elements (S, Pb), "first category" trace elements (Fe, Zn, Sb, Ag, Cu, Mn, Ni, Cd, Sr), and "second category" trace elements (Co, Bi, Hg, As, Au, Se).

Taking into account the stoichiometric composition of galena (86.4% Pb, 13.6% S) a study was made of the deviation of each sample from the theoretical galena composition (Fig. 7). For this purpose, in each sample the sum of the contents of all elements analyzed was plotted with respect to the lead content. The distribution of most of the analytical data is around the theoretical value, showing a narrow but erratic dispersion of data, with the exception of type E deposits. All the type E data show a distribution that can be adjusted to a straight line with a positive slope. The composition of galena concentrates from type E deposits is below the theoretical composition of galena, indicating that they are not pure galena and that the trace elements form micro-inclusions of different mineral phases. The quantity and composition of galena micro-inclusions is probably a linear function corresponding to the aforementioned straight line.

The data and most important statistical parameters are given in Table 4 and the correlation matrix is shown in Table 5. Some correlation values are very high: above 0.9 for Se–Bi and Se–Hg; between 0.8 and 0.9 for Sb–Co and As–Bi; and between 0.7 and 0.8 for Fe–Ag, Fe–Bi, Zn–Cd, Sb–Ag, Ag–Co, Cu–Hg, Cu–Se and As–Se. The Zn–Cd correlation is due to the presence of sphalerite and the Sb–Ag correlation is due to the presence of Ag antimonides and sulfo-antimonides. The positive correlation between Sb–Co, Sb–Ag and Ag–Co indicates that the three elements are probably associated with several mineral phases such as linneite and sulfosalts. The close cor-

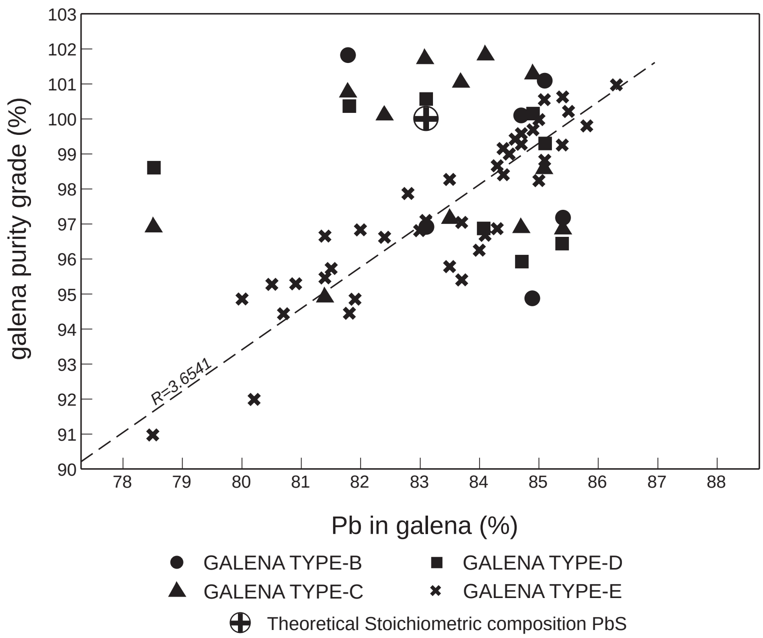

Fig. 7. Scatter diagram between Pb content and grade of purity of galena (determined from the sum of the elements analyzed in concentrates from Alcudia Valley mineral field). The dotted line is the regression straight for type E deposits only.

Table 4
Analytical data of galena concentrates from the Alcudia Valley mineral field deposits

Mine or occurrence	Major elements			Trace elements 1st category							Trace elements 2nd category					
	Pb (%)	S (%)	Fe (%)	Zn (ppm)	Sb (ppm)	Ag (ppm)	Cu (ppm)	Mn (ppm)	Ni (ppm)	Cd (ppm)	Sr (ppm)	Co (ppm)	Bi (ppm)	Hg (ppm)	As (ppm)	Au (ppm)	Se (ppm)
Type B deposits																	
Eufrasia	82.00	14.49	0.17	4404	430	360	4014	48	3	25.4	2	5	110	110	<0.5	<3	1500
Los Diegos	85.90	15.16	0.04	7788	130	88	5	5	14	33.7	2	2	<5	11	<0.5	36	46
San Bartolomé	79.80	14.29	0.14	8279	350	340	447	32	2	28.2	2	7	12	32	<0.5	<3	390
San Benito	87.70	13.33	0.07	380	500	480	608	32	4	8.0	2	2	7	12	<0.5	9	46
Santa Isabel (Filón Sur)	85.20	14.87	0.03	389	1300	800	346	5	10	10.8	2	1	<5	28	<1	27	40
Atilana	81.70	15.16	0.06	3189	610	480	245	5	2	19.2	2	4	<5	11	<0.6	<5	88
Mean	83.72	14.55	0.09	4072	553	425	944	21	6	20.9	2	4	43	34	0.0	24	352
Standard deviation	3.01	0.69	0.06	3452	400	233	1517	19	5	10.1	0	2	58	38	0.0	14	579
Type C deposits																	
Navalahiguera	86.30	14.97	0.02	4570	360	200	70	21	10	13.6	3	3	<5	9	<0.5	<2	9
Virgen del Socorro	86.40	14.29	<0.01	604	1100	920	311	5	2	7.2	7	<1	<5	27	<0.7	16	230
El Contadero	85.70	15.54	0.05	432	1300	690	245	5	8	7.3	2	<1	<5	12	<1	<5	32
Las Minillas	83.60	14.59	0.07	3946	230	180	322	20	2	7.4	2	2	<5	19	<0.5	15	130
El Músico	81.10	15.73	0.33	840	1700	480	2628	30	781	8.6	2	12	<5	19	110.0	<8	45
Navalajeta	82.3	14.49	<0.02	759	960	410	264	5	140	6.9	3	1	9	8	<0.7	12	28
Mean	84.23	14.94	0.12	1859	942	480	640	14	157	8.5	3	5	9	16	110.0	14	79
Standard deviation	2.24	0.59	0.14	1874	561	287	978	11	310	2.6	2	5	0	7	0.0	2	85
Type D deposits																	
Arroyo del Royar	86.10	14.49	0.14	637	320	200	143	17	6	10.8	2	1	<5	11	<0.5	<2	32
Las Simonas	85.10	14.87	0.08	4580	350	210	7	5	3	41.2	4	2	<5	29	<0.5	<2	24
Nacedero	86.70	13.48	0.10	540	1700	780	78	30	5	14.0	2	<1	<5	<2	<1.1	49	34
Las Perras	85.50	13.81	0.03	33	440	410	7	5	2	36.5	16	1	<5	24	<0.5	<3	23
Fajano	80.90	15.06	0.08	549	600	290	103	33	5	27.2	3	<1	15	10	<0.6	44	13
Navalcaballejo	81.70	14.49	0.15	3228	430	300	37	49	6	35.8	2	2	10	21	<0.5	<3	28
Tres Ventas	83.80	14.28	0.05	5554	2000	840	433	5	2	36.3	4	<1	<5	31	<1.3	28	50
Pepita	82.30	14.5	0.03	1056	630	460	663	30	2	27.6	2	<1	<5	11	6.3	115	23
Mean	84.01	14.37	0.08	2022	809	436	184	22	4	28.7	4	2	13	20	6.3	59	28
Standard deviation	2.17	0.52	0.05	2126	657	248	238	16	2	11.1	5	1	4	9	0.0	38	11
Type E deposits																	
Cerro Verde	80.50	14.77	0.15	39	3100	850	130	43	46	3.3	2	3	8	13	42.0	<21	48
Diógenes	82.40	14.22	0.58	64	4900	1900	39	195	154	2.6	2	17	18	<7	76.0	<36	<18

Diógenes	82.80	15.06	0.23	120	7600	2300	293	132	269	3.3	4	27	<5	<11	<5.7	<48	<23
El Campillo	84.30	12.57	<0.02	22	1400	170	74	5	2	3.1	116	4	8	10	<0.9	<7	<5
El Horcajo	80.20	11.80	1.21	81	3400	2800	289	5	2	2.2	8	<1	<5	<4	<2.3	<18	<8
Emperatriz	83.70	11.70	<0.02	52	1400	170	23	10	6	1.2	174	<1	<5	<2	<1.1	<7	<5
Felisa	83.00	13.81	0.13	71	3300	340	796	8	12	1.0	4	3	7	14	<1.8	<19	<10
Fonógrafo 2°	84.00	12.26	0.22	40	2900	270	96	15	14	3.3	45	7	13	38	<2.3	<27	<7
La Boticaria	84.70	14.87	0.11	119	2600	320	290	5	11	3.6	5	2	<5	15	<1.9	<15	<7
La Boticaria	85.40	15.16	0.10	761	2000	230	255	17	16	7.3	8	2	<5	8	<1.3	<8	11
La Fama	85.00	13.24	<0.04	60	2800	290	1878	17	7	2.9	56	<1	<5	42	<1.7	28	31
La Fortuna	80.00	14.87	0.12	31	740	76	69	26	5	2.2	2	<1	14	8	<0.7	<5	<3
La Gitana	84.40	14.01	0.33	36	4300	430	2423	5	15	2.5	2	<1	10	20	<2.4	<19	<9
La Jarosa	85.40	13.85	0.03	123	930	160	50	49	2	0.9	2	3	8	8	6.6	<4	7
La Petaca	81.40	15.25	<0.02	61	540	140	492	21	49	1.8	2	5	18	8	<0.6	13	<3
La Romanilla	81.50	14.22	0.12	106	2100	300	259	63	50	1.5	13	8	<5	<2	<1.2	<9	<6
La Salvadora	80.70	13.75	0.13	44	4200	1300	489	29	91	1.1	2	15	8	<5	160.0	<24	<11
La Veredilla	85.10	13.72	0.05	51	1900	200	201	5	7	3.3	135	2	<5	15	<1.2	<8	<5
La Victoria	84.90	14.77	0.29	133	4700	3400	1139	16	2	5.4	2	8	61	<5	0.8	<27	<14
María Aurora	83.50	14.77	0.30	107	2100	110	20	23	10	3.0	3	<1	<5	7	<1.7	<17	22
Pje. Cañadahonda(836-55)	84.70	14.58	0.08	47	770	56	26	35	21	2.4	22	2	<5	5	<0.7	<4	<5
Pje. Cañadahonda(836-57)	83.50	12.28	<0.02	50	2100	180	429	10	9	6.4	140	<1	<5	19	<1.3	<8	<5
Pje. Cañadahonda(836-58)	84.10	12.57	0.10	65	3100	430	1558	37	16	2.9	101	3	<5	<4	<2.3	<17	<7
Pje. Encinarejo (836-59)	81.90	12.95	0.07	49	2000	270	320	29	6	6.4	123	3	<5	17	<1.9	<14	<6
Pje. Encinarejo (836-66)	84.50	14.49	<0.05	83	2900	450	1856	31	12	3.6	23	<1	6	<4	<1.7	<18	<10
Pje. Moroteras (835-116)	85.10	15.45	<0.01	19	540	130	22	5	12	3.0	15	1	<5	11	<0.5	10	<3
Quinto del Río	85.80	14.01	0.05	24	520	150	164	5	3	4.9	44	<1	<5	9	<0.5	<2	5
Rica Nueva	84.30	14.29	0.05	790	890	140	91	5	7	5.6	7	2	<5	10	<0.8	<5	8
San José	84.60	14.77	<0.05	454	3400	240	205	37	142	5.6	16	<1	8	<4	<2.2	<16	<10
San Quintín (D. Raimundo)	85.50	14.68	0.10	437	2500	1200	240	12	14	8.1	2	<1	<5	9	<1.1	<9	<5
San Quintín (San Froilán)	82.00	14.50	0.16	3328	3300	1400	507	22	5	27.6	2	<1	8	<4	<2.2	<21	<10
San Serafín	78.50	12.47	1.37	21	3000	2300	283	5	111	1.7	11	8	<5	5	170.0	<17	<7
Santa Bárbara	84.40	14.68	0.02	765	1500	220	50	5	7	19.2	2	<1	6	<2	<1.1	<7	<5
Santa Rosa	85.00	14.97	<0.08	52	5200	2000	99	5	7	2.8	2	<2	8	<7	<3.9	<30	<14
Santa Teodora	80.90	14.39	<0.02	130	1000	110	46	21	36	3.5	2	<1	<5	7	<0.8	<6	7
Villagutiérrez (Alberto)	81.40	14.03	0.88	369	4900	3700	1249	21	11	4.0	2	19	952	<5	290.0	<26	<12
Villagutiérrez (Buenpento,)	86.30	14.68	<0.05	40	3400	2000	21	33	16	5.8	2	<1	<5	<4	15.0	<19	<10
Villalba	83.70	13.33	<0.02	94	1400	110	552	16	3	3.7	58	2	12	16	<0.8	24	<5
Mean	83.40	13.99	0.27	235	2614	812	448	27	32	4.5	31	7	65	14	95.1	19	17
Standard deviation	1.91	1.02	0.35	557	1571	1008	596	36	54	4.9	48	7	222	9	102.9	9	15

Samples were analyzed by ICP/MS and S by LECO at Actlabs laboratories (Canada).

Table 5
Correlation matrix between trace elements in galena concentrates from the Alcudia Valley mineral field

	Pb	S	Fe	Zn	Sb	Ag	Cu	Mn	Ni	Cd	Sr	Co	Bi	Hg	As	Au	Se
Pb	1.00000																
S	.11410	1.00000															
Fe	−.49811	−.42540	1.00000														
Zn	−.04823	.26818	−.19138	1.00000													
Sb	−.12128	−.09313	.46451	−.35353	1.00000												
Ag	−.18446	−.04993	.71267	−.14709	.71268	1.00000											
Cu	−.12050	.01599	.13169	.06263	.16175	.07779	1.00000										
Mn	−.19592	.09922	.10789	−.06415	.40648	.22774	.03510	1.00000									
Ni	−.25319	.24225	.18672	−.08515	.21688	.10044	.30637	.29866	1.00000								
Cd	.02024	.26447	−.27878	.72630	−.39527	−.14590	−.00945	−.09738	−.11691	1.00000							
Sr	.00324	−.65747	−.13016	−.23296	−.07556	−.24415	−.04374	−.11845	−.12086	−.24174	1.00000						
Co	−.44246	.03077	.48617	−.14868	.80750	.71391	.19372	.64185	.46475	−.25097	−.17584	1.00000					
Bi	−.16536	−.01849	.77131	−.03621	.27714	.61615	.20868	−.05385	−.10581	−.07974	−.08699	.59662	1.00000				
Hg	−.03038	−.07270	−.03389	.34591	.00688	.01885	.71398	.24410	−.03051	.34102	−.05088	.20341	.41856	1.00000			
As	−.58593	−.18613	.69061	.00118	.49142	.51093	.32138	−.10771	.17968	−.28664	−.24044	.70415	.83790	.03437	1.00000		
Au	−.24906	−.01248	−.30344	.04811	.00126	.11852	.07349	.43446	−.26470	.55045	−.12005	−.11275	.42588	−.10185		1.00000	
Se	−.22027	.01513	.23171	.33578	−.17583	.05265	.75191	.34996	−.05719	.18829	−.09581	.27055	.95634	.90647	.75577	−.36156	1.00000

relation between the other elements could not be interpreted as elements included in the galena framework, because, as in the case of sphalerite, the correlation indices between the "first category" trace elements and the major elements (S and Pb) are low.

The characteristics of each type of deposit in relation to trace elements in galena are summarized as follows: galena from type B deposits is relatively rich in Bi, Hg and Se, and has some Au; galena from type C deposits is rich in Ni and Se, with some Au; galena from type D deposits is rich in Cd, Hg and Se, and its Au content is the highest of all types; and galena from type E is rich in Ag, Sb and Sr and does not contain any Au.

Since the number of analyzed samples differs greatly between ore types, it is not possible to compare directly the data among them. In order to achieve such a comparison, a weighted function was created to allow us to obtain a comparable value for each type. The weighted function for an element "*e*" from a specific deposit type is:

$$\mathrm{Ve}_{\mathrm{weighted}} = \left[\left(\mathrm{Xe}_{\mathrm{weighted}}\right)*10 - d^2\right]*\mathrm{Re}$$

$\mathrm{Ve}_{\mathrm{weighted}}$ is the weighted value obtained for the element "*e*". $\mathrm{Xe}_{\mathrm{weighted}}$ is the weighted average of element "*e*". d^2 is the standard deviation of element "*e*". Re is the representativeness of the element in the type and is the quotient of the number of analyzed cases above the detection limit and the total number of cases. The $\mathrm{Xe}_{\mathrm{weighted}}$ is multiplied by 10 to avoid obtaining negative values and to emphasize the average value. The average and standard deviations are only taken into account for values above the detection limits.

The values $\mathrm{Ve}_{\mathrm{weighted}}$ obtained with this function are plotted in Fig. 8A and B. Both graphs enable comparison of the behaviour of trace elements in the vein ore types.

First-category trace elements (Fig. 8A) show a similar behavior in the three syntectonic deposit types (B, C and D), except for Ni in type C deposits. In the case of the post-tectonic (type E) deposits Zn, Ni and Sr show different behavior than in the other groups (Fig. 8A). In the case of the second category trace elements the three types of syntectonic deposits again show the same behavior, the tendency in the case of B and D being practically the same. Again, the

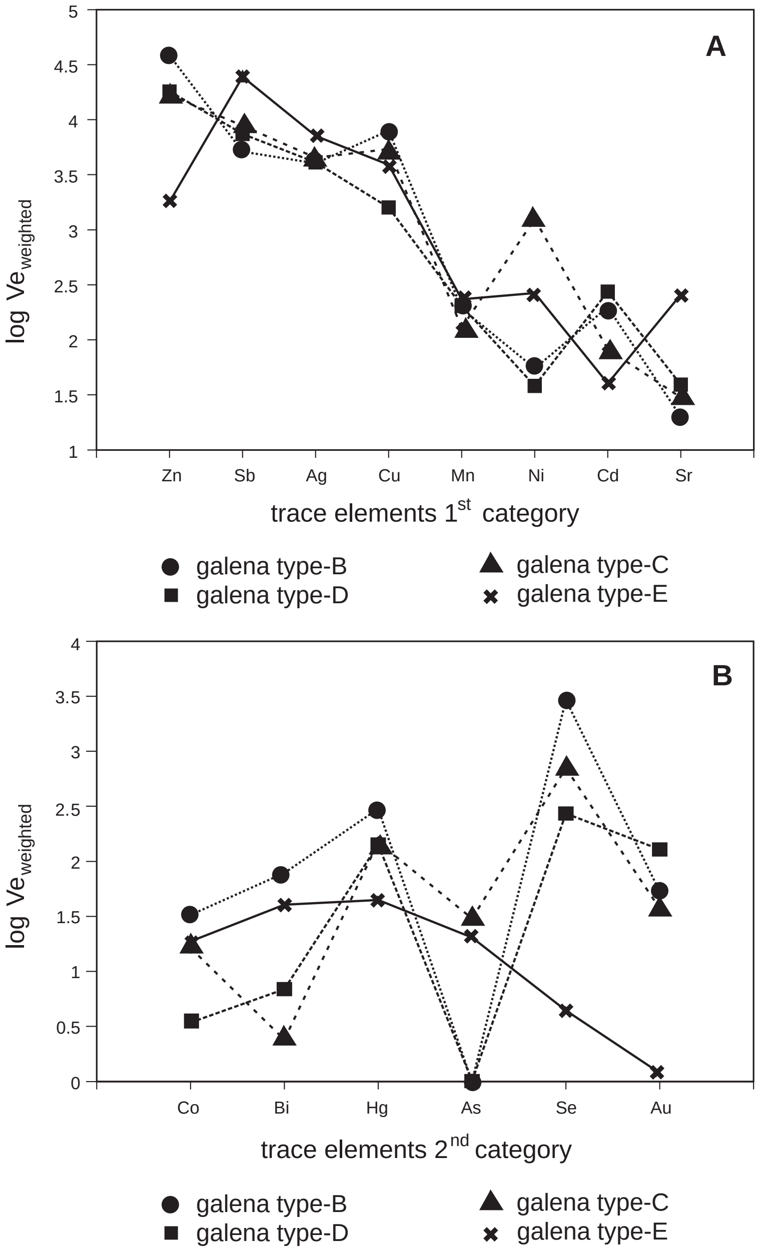

Fig. 8. Variation of $Ve_{(weighted)}$ value calculated for the trace elements of galena concentrates of Alcudia Valley mineral field. $Ve_{(weighted)}$ values were calculated for each element taking into account the average weighting of the number of cases over the detection limit, the standard deviation and a factor as a function of the representativeness of the element (see explanation in text).

type E deposits line is very different from the other groups. In conclusion, Types B and D galena have approximately the same behavior, and only type B is rich in Cu. Both types of deposits are located in shear zones and, according to Palero (1986, 1991), Delgado et al. (1988) and Palero et al. (1992), were formed during the shear development. The behavior of galena from type C is close to types D and B except for Cd,

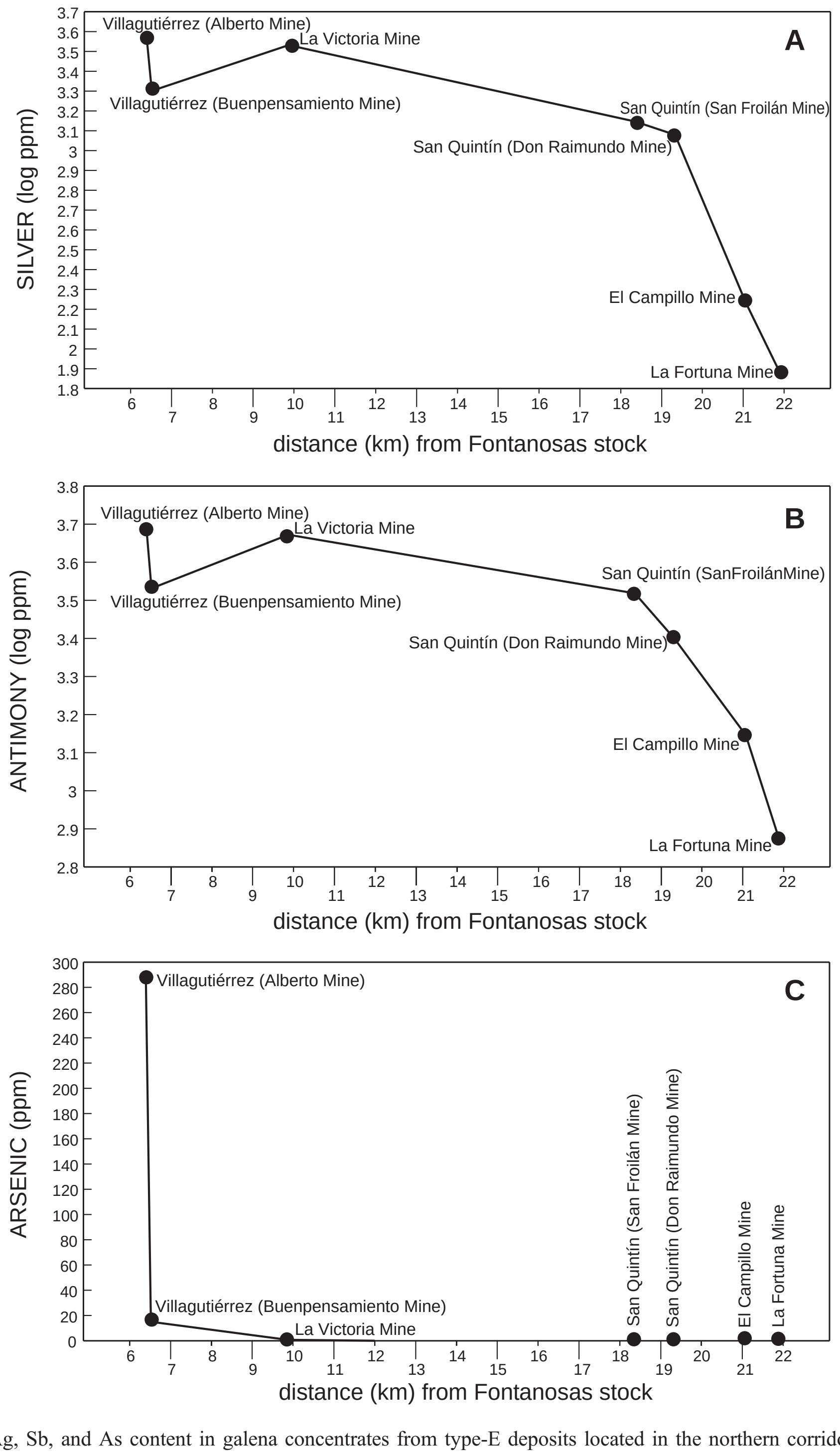

Fig. 9. Variation of Ag, Sb, and As content in galena concentrates from type-E deposits located in the northern corridor (see Fig. 4) versus distance to Fontanosas pluton and the sub-outcropping El Moto cupola.

Ni, Bi and As. In both graphs galena from type E differs significantly from other types, and could be interpreted as having resulted from different conditions of formation.

The existence of three silver corridors for type E deposits suggests that the content of an element in galena concentrates should be a function of the geographic position of the deposit relative to these corridors. To investigate this, deposits of type E have been plotted in UTM geographic coordinates and the axis of each corridor has been calculated as the regression straight line of these UTM points. In Figs. 9 and 10 the analytical data of galena concentrates from deposits within each corridor are plotted as a function of the distance from the igneous rocks and from the axis of the corridor.

For the northern corridor, the Ag and Sb contents versus the distance to the Fontanosas pluton are plotted in Fig. 9A and B. A gradual decrease is seen as far as the San Quintin deposit followed by a rapid fall to the end of the corridor. As is intimately related to the vicinity of igneous rocks and is only detected in the galena concentrate from the deposit close to the granite stock (Fig. 9C).

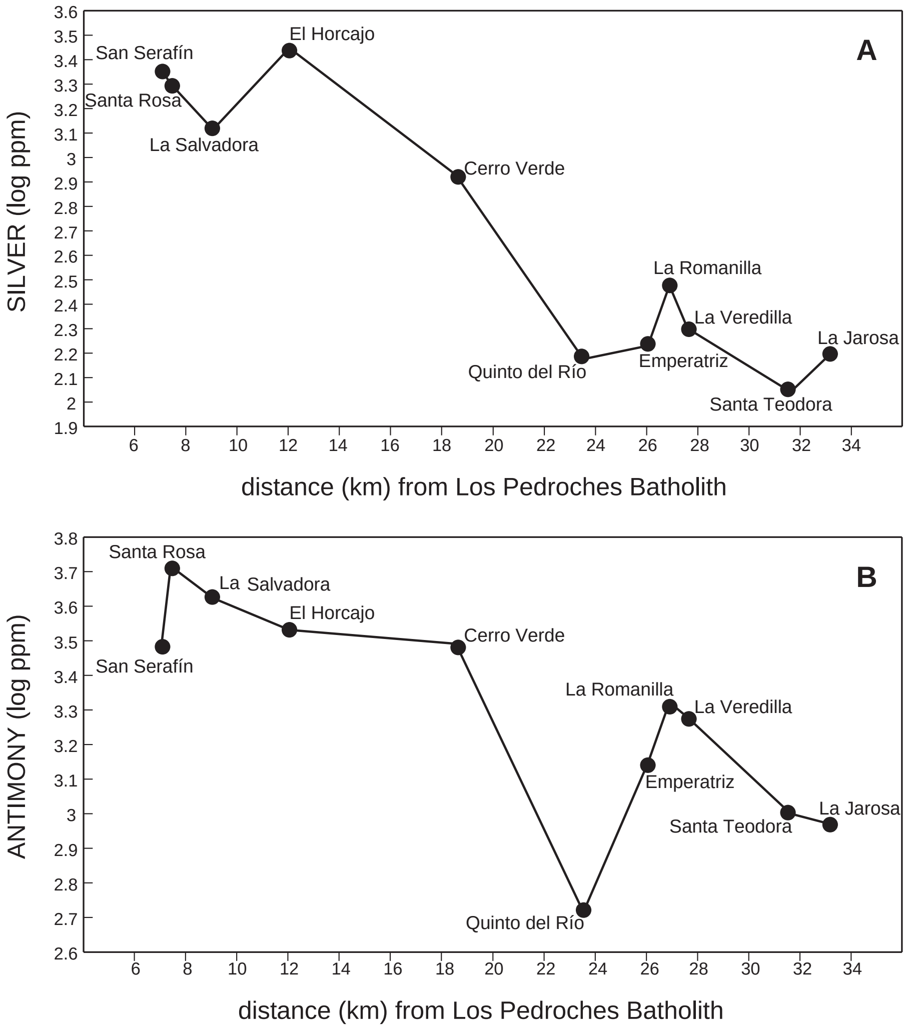

Fig. 10. Variation of Ag, and Sb content in galena concentrates from type E deposits located in the western corridor (see Fig. 4) versus the distance to Los Pedroches Batholith.

In the western corridor Ag and Sb are plotted versus the distance from the Los Pedroches batholith (Fig. 10). Both elements decrease in concentration away from the granite, but the behavior of Ag is somewhat different from the previous corridor in that it decreases from the first to the third deposit and then increases in the fourth (Fig. 10A). The mineral associations in the first three have abundant Ag-rich sulfosalts in the form of individual grains with a fairly large grain size (freibergite, bournonite and boulangerite) and, as the concentrates are of high purity galena, the Ag content in galena is lower than expected. By contrast, at El Horcajo, the fourth deposit, only sulfosalts are present in very fine grain size, usually in the form of micro-inclusions in galena. Furthermore, microprobe testing shows that part of the Ag is in the galena framework. Sb concentrations (Fig. 10B) decrease progressively with very little variation with the exception of the Quinto del Rio deposit, which is so anomalous that it suggests that either a sampling error occurred, or that it lies too far from the axis of the corridor (see Fig. 4).

In the eastern corridor the results are inconclusive, probably due to an inadequate number and distribution of samples. In this corridor galena concentrates were obtained only from samples from the Diogenes mine, located in the middle of the corridor, and other samples came from the end of the corridor.

In conclusion, Ag in galena from type E deposits shows the same type of zonation as Ag in the bulk ore. This zonation has a regional character indicating that type E deposits are related to the granitic intrusions, in agreement with conclusions of Palero et al. (2003) and García de Medinabeitia (2003).

5. Discussion and conclusions

The Pb–Zn deposits of the Alcudia Valley mineral field have a heterogeneous metallogeny, with five different ore deposit types (Palero, 1991). These five types reflect five mineralizing processes that can be related to different stages of the Hercynian Orogeny and could be distinguished as either pretectonic, syntectonic or post-tectonic (Palero et al., 2003). Three of the five mineralization types are syntectonic with vein morphology. Each type is related to different hydrothermal processes during the Hercynian Orogeny. The post-tectonic deposits are also veins and were economically the most important. They were formed during regional-scale hydrothermal circulation related to cooling of the Hercynian granitoids (Palero et al., 2003; García de Medinabeitia, 2003).

In the Alcudia Valley, trace elements in sphalerite concentrates provide an excellent tool to differentiate among the five different types of ore deposits. Cd, Sb, Ag, Cu and Co are the best elements to distinguish the deposit types. In scatter diagrams of pairs of these five elements, different deposit types plot separately (Figs. 5 and 6), and the separation between syntectonic and post-tectonic deposits is very clear. In general, type E deposits are characterized by a high trace element content, especially Cd, Ag and Sb, and type C is very poor in trace elements.

Trace elements in galena concentrates are also a good guide for differentiating between deposit types. As a general rule, type B galena concentrates are rich in Cu, Bi, Hg and Se; type C in Se and Ni; type D in Cd and Au; and type E in Ag, Sb, Sr and Ni. The comparative analyses of the weighted data of trace elements from galena (value $Ve_{weighted}$) indicate that galena concentrates from type B and D are very similar, galena concentrates from type C are close to types B and D (except for Ni and Bi), and galena concentrates from type E are quite different. Again the difference between the syntectonic and post-tectonic deposits is clear.

Statistical analysis of element correlations indicates high values between Cd–Ag, Cd–Sb, Ag–Sb and In–Sn in sphalerite and Se–Bi, Se–Hg, Sb–Co, As–Bi, Fe–Ag, Fe–Bi, Sb–Ag, Ag–Co, Cu–Hg, Cu–Se and As–Se in galena. Because these trace elements exhibit low correlations with the major elements in sphalerite (Zn and S) and galena (Pb and S), they are probably present as micro-inclusions in the sulfides. The high negative correlation between Zn and Fe in sphalerite indicates their mutual substitution in the sphalerite crystal lattice. The high positive correlation between Zn and Cd in galena suggests that both elements are present as sphalerite micro-inclusions in galena.

Ag in the bulk ores of type E deposits shows a regional zonation, decreasing outward from the granite bodies in three corridors and decreasing outward from the center of each corridor. The Ag distribution coincides with the paragenetic zonation of type E deposits (Palero and Martín-Izard, 1992; Palero et al., 2003). This zonation is also detectable in the trace element contents in galena, being most clear in the case of Ag, Sb and As, but can only be detected on a broad scale and is not observable when only a few deposits are studied.

The different patterns of trace elements in sphalerite and galena are coincident with the classification of deposit types and are probably a direct consequence of different mineralizing processes. In this regard, Hall and Heyl (1968) and Viets et al. (1992) reported differences in trace element contents in Pb–Zn ores from different mining districts, but all the deposits studied belong to a single model, the Mississippi Valley type. Hall and Heyl (1968) also found poorly-defined zonation, particularly in Ag and Sb, with regard to the supposed mineralizing focus (feeders) in the Illinois–Kentucky district. Viets et al. (1992) demonstrated a clear influence of the host rocks in the mineralizing processes, with some trace elements (Cu, Ga and Ge in sphalerite) characteristic of that phenomenon.

Based on the genetic models established by Palero et al. (2003) and the lead isotope data from García de Medinabeitia (2003), a relationship has been established between trace element contents in galena and sphalerite and the complexity and importance of the hydrothermal systems that formed the deposits. Thus, the most important hydrothermal phenomenon was formation of the post-tectonic (type E) deposits, in which sphalerite and galena are strongly enriched in trace elements. Either granitoids or metasedimentary rocks could be the source of the trace elements. The regional zonation suggests that some elements, such as As, came from the Hercynian granitoids (Štemprok, 1978 and Stone, 1982), and the physico-chemical conditions such as temperature (higher close to the igneous rocks) controlled the precipitation of some elements like Ag or Sb.

Types B and D deposits are syntectonic and directly related to the development and dynamics of shear zones. It is interesting to note that Au, an element typically mobilized into shear zones, was detected in some of the galena concentrates from these types of syntectonic deposit.

The main control in the formation of the Alcudia Valley deposits was structural, but the development of structures during orogenic activity was strongly controlled by the lithostratigraphic units (see Fig. 3). Consequently, the host rocks of the deposits exerted a strong influence on the chemistry of these deposits (Palero, 1991; Palero et al., 2003). In this respect, sphalerite is more sensitive indicator than galena, particularly using Cd and Cu, and allows the deposits located in the Palaeozoic and Precambrian rocks to be differentiated geochemically.

In conclusion, the study carried out in the Alcudia Valley mineral field suggests that trace element analyses of sphalerite and galena can be used as a tool to differentiate various types of deposits in a region. Sphalerite appears to be more useful for this purpose than galena, but the latter may show regional distribution patterns that could be exploited as an aid in the exploration of Zn–Pb mining districts.

Acknowledgements

This manuscript has been much improved through detailed comments and helpful suggestions by R. Both, A. Arribas Jr, S. Dewaele and S. Kesler. The work was financed by the Oviedo University Project df-93-215-43 and MCYT project BTE 01-3469 (Spanish Ministry of Science and Technology).

References

Álvarez Nava, H., García Casquero, J.L., Gil Toja, A., Hernández Urroz, J., Lorenzo Álvarez, S., Lorenzo Díaz, F., Mira López, M., Monteserín, V., Nozal, F., Pardo, M.V., Picart, J., Robles, R., Santamaría, J., Solé, F.J., 1988. Unidades litoestratigráficas de los materiales precámbrico–cámbricos en la mitad suroriental de la Zona Centro-Ibérica: II. Comunicaciones, vol. 1. Congreso Español de Geología, Granada, pp. 19–22.

Amor, J.M., Ortega E., 1987. Memoria explicativa de la hoja n° 809, Tirteafuera. Mapa Geológico de España, escala 1:50000. 2ª serie, plan MAGNA. IGME.

Ancoechea, E., 1983. Evolución espacial y temporal del vulcanismo reciente de España Central. PhD thesis. Universidad Complutense de Madrid, Spain. 657 pp.

Arribas Moreno, A., 1981. Distribución geoquímica de los elementos en trazas de los yacimientos españoles del tipo B.P.G.C. Fundación Juan March. Serie Universitaria 146, 1–54.

Arribas Moreno, A., Arribas Rosado, A., Gumiel Martínez, P., Martín Izard, A., Reguilón Bragado, R., 1988. Caracteres metalogénicos de los yacimientos minerales asociados a los granitoides del Macizo Hespérico. In: García de Figuerola, L.C. (Ed.), Libro Jubilar. Rueda, pp. 233–263.

Bauchau, C., 1971. Essai de typologie quantitative des gisements de plom et zinc avec la réparttion de ĺaggent. Bulletin de B.R.G.M., nums. 3, 1–72, and 4, 1–43.

Beaudoin, G., Sangster, D.F., 1992. A descriptive model for the silver–lead–zinc veins in clastic metasedimentary terranes. Economic Geology 87, 1005–1021.

Bouyx, E., 1970. Contribution a l'etude des formations ante-Ordoviciennes de la meseta meridionale Ciudad Real et Badajoz. Memoria del Instituto Geológico y Minero de España 73, 1–263.

Castroviejo, R., 1979. Génesis de los indicios Zn–Pb en el Ordovícico de la cuenca del río Ojailén (Puertollano-Ciudad Real): aportación del estudio mineralógico-textural. Boletín de la Sociedad Española de Mineralogía 1E, 31–41.

Coupez, Y., Tomkinson, M., Phillips, A., 1988. Use of correlations between structural analysis of outcrop, remote sensing and gravity data to aid exploration for base metal mineralization in the Almadén region of Spain. 2nd Remote Sensing European Workshop, Bruxelles, 1986, pp. 177–242.

De Gyves, J., 1988. Determinación de elementos menores y traza por fluorescencia de rayos-X en esfalerita. PhD thesis. Universidad Autónoma de Barcelona, Spain. 204 pp.

Defalque, G., Demaiffe, D., Dumont, P., Lalieux, P., 1992. Le batholite de Los Pedroches Sierra Morena. Études cartographique, pétrographique, géochimique, géochronologique et métallogénique. Annales de la Société Géologique de Belgique 3 (1–2), 333–350.

Delgado, J.C., Martín-Izard, A., y Palero, F.J., 1988. Litogeoquímica de la formación Estratos Pochico Ordovícico Inferior y su relación metalogénica con algunos yacimientos filonianos de Pb–Zn de Sierra Morena Oriental. Geociencias 3, 333–350.

Díez Balda, M.A., Vegas, R., González-Lodeiro, F., 1990. Central-Iberian Zone. Structure. In: Dallmeyer, R.D., Martínez García, E. (Eds.), Pre-Mesozoic Geology of Iberia. Springer-Verlag, pp. 172–188.

Donaire, T., Pascual, E., 1992. Caracterización petrológica y geoquímica del sector central del batolito de los Pedroches: discriminación de dos series de granitoides. Revista de la Sociedad Geológica de España 5, 41–54.

Gallardo, J.L., Gomis, E., Dinarés, J., Pérez-González, A., 1998. Relaciones entre las polaridades paleomagnéticas y las edades radiométricas del volcanismo del Campo de Calatrava Ciudad Real. Geogaceta 23, 55–58.

García de Medinabeitia, S., 2003. Implementación y aplicación de los análisis isotópicos de Pb al estudio de las mineralizaciones y la geocronología del área Los Pedroches-Alcudia (Zona Centro-Ibérica). PhD thesis Universidad del País Vasco, Spain. 207 pp.

García Sansegundo, J., Lorenzo Álvarez, S., Ortega, E., 1987. Memoria explicativa de la hoja n° 808, Almadén. Mapa Geológico de España, escala 1:50,000. 2ª serie, plan MAGNA. IGME.

Hall, W.E., Heyl, A.V., 1968. Distribution of minor elements in ore and host rock, Illinois–Kentucky District and Upper Mississippi Valley zinc–lead district. Economic Geology 63, 655–670.

Higueras, P., Acosta, A., 1992. Alteración de materiales volcánicos paleozoicos en el sinclinal de Almadén. Actas de las reuniones científicas: III. Congreso Geológico de España. XII Reunión de la SEM. Salamanca 3, pp. 143–147.

Julivert, M., Ribeiro, A., Conde, L., 1972. Memoria explicativa del Mapa Tectónico de la Península Ibérica y Baleares, Escala 1:100,000. IGME.

Kretz, R., 1983. Symbols for rock forming minerals. American Mineralogist 68, 277–279.

Larrea, F.J., Carracedo, M., Alonso, A., Ortega, L.A., and Minéndez, M., 1999. Granitoides postcolisionales en situaciones extensionales: el plutón de Cardeña-Virgen de la Cabeza (batolito de Los Pedroches, España): XV. Reunión de Geología del Oeste Peninsular-International Meeting on Cadomian Orogens, 159–169.

Leal Echevarría, G., Capote, R., Galán, E., Hernández Enrile, J.L., 1976. Génesis de las mineralizaciones del área Pedroches-Linares en relación con la evolución geotectónica del cinturón hercínico de Sierra Morena Oriental. Fundación Juan March, 195 pp. (Unpublished report).

Leutwein, J., Saupe, F., Sonet, J., Bouyx, E., 1970. Première mesure géochronologique en Sierra Morena: la granodiorite de Fontanosas Ciudad Real, Espagne. Geologie en Mijnbouw 49, 297–304.

Neiva, A.M.R., 1982. Geochemestry of muscovite and some physico-chemical conditions of the formation of some tin–tungsten deposits. In: Evans, A.M. (Ed.), Metallization Associated with Acid Magmatism, vol. 6. John Wiley and Sons, Ltd., pp. 243–259.

Ortega, E., 1988. Geology and Metallogeny of the Almadén area, Centroiberian zone, Spain. 2nd Remote Sensing European Workshop Bruxelles, 1986, 149–173.

Ortega, E., González-Lodeiro, E., 1986. La discordancia intra-Alcudiense en el dominio meridional de la zona Centroibérica. Breviora Geológica Astúrica 27, 27–32.

Ortega, E., Hernández Urroz, J., González Lodeiro, F., 1988. Distribución paleogeográfica y control estructural de los materiales anteordovícico en la parte suroriental del autóctono de la zona Centroibérica. II Congreso Nacional de Geología, Simposio sobre Cinturones Orogénicos. Granada, pp. 85–89.

Palero, F.J., 1986. El campo filoniano de El Hoyo de Mestanza. (Ciudad Real). Sobre el origen de las mineralizaciones B.P.G.C. asociadas a zonas de cizalla. Stvdia Geologica Salmanticensia 23, 265–297.

Palero, F.J., 1991. Evolución geotectónica y yacimientos minerales de la Región del Valle de Alcudia, (Sector Meridional de la Zona Centroibérica). PhD thesis Universidad de Salamanca, Spain. 827 pp.

Palero, F.J., 1992. La sucesión paleozoica y estructura del sinclinal de Solana del Pino Ciudad Real. Estudios Geológicos 48, 209–381.

Palero, F.J., 1993. Tectónica pre-hercínica de las series infraordovícicas del anticlinal de Alcudia y la discordancia intraprecámbrica en su parte oriental Sector meridional de la Zona Centroibérica. Boletín Geológico y Minero 104, 227–242.

Palero, F.J., Martín-Izard, A., 1988. Las mineralizaciones estratoides de Zn–Pb en la Caliza Urbana del paraje de Peña del Aguila, Calzada de Calatrava Ciudad Real. Boletín de la Sociedad Española de Mineralogía 11, 179–189.

Palero, F.J., Martín-Izard, A., 1992. Contenido en Ag de las mineralizaciones de Pb–Zn de la región del Valle de Alcudia Ciudad Real: implicaciones en la génesis de yacimientos hidrotermales de metales base. III Congreso Geológico de España y XII Reunión de la Sociedad Española de Mineralogía, Salamanca, vol. 3, pp. 252–257.

Palero, F.J., Both, R.A., Mangas, J., Martín-Izard, A., Reguilón Bragado, R., 1992. Metalogénesis de los yacimientos de Pb–Zn de la región del Valle de Alcudia Sierra Morena Oriental. In: García Guinea, J., Martínez Frías, J. (Eds.), Recursos minerales de España. Textos Universitarios, vol. 15. C.S.I.C., Madrid, pp. 1027–1067.

Palero, F.J., Both, R.A., Arribas, A., Boyce, A.J., Mangas, J., Martín-Izard, A., 2003. Geology and metallogenic evolution of the polymetallic deposits of the Alcudia Valley mineral field, Eastern Sierra Morena, Spain. Economic Geology 98, 577–605.

Penha, M.H., Arribas, A., 1974. Datación geocronológica de algunos granitos uraníferos españoles. Boletín Geológico y Minero 85, 271–273.

Peran, M., Tamain, G., 1967. La "Formación Campana" dans le nord de la province de Jaén Espagne. Comptes Rendus de l'Academie des Sciences, vol. 265. Paris, pp. 844–847.

Pérez Lorente, F., 1979. Geología de la zona Ossa-Morena, al norte de Córdoba (Pozoblanco-Bélmez-Villaviciosa de Córdoba). PhD thesis Universidad de Granada, Spain. 330 pp.

Plant, J.A., Simpson, P.R., Green, P.M., Watson, J.V., Fowler, M.B., 1983. Metalliferous and mineralized Caledonian granites in relation to regional metamorphism and fracture systems in northern Scotland. Transactions of the Institution of Mining Metallurgy. Sect. B: Applied Earth Sciences 92, 33–42.

Ribeiro, A., 1974. Contribution a l'etude tectonique de Tras-Os-Montes oriental, vol. 24. Serviço Geológico de Portugal, pp. 1–168.

Rodríguez Pevida, L., Mira, M., Ortega, E., 1990. Memoria explicativa de la hoja n° 833, Hinojosa del Duque. Mapa Geológico de España, escala 1:50000. 2ª serie, plan MAGNA. IGME.

Roiz, J.M., 1979. La estructura y la sedimentación herciniana, en especial el Precámbrico superior, en la región de Ciudad Real-Puertollano. PhD thesis, Universidad Complutense de Madrid, Spain, 236 pp.

Rundquist, D.V., 1982. Zoning of metallization associated with acid magmatism. In: Evans, A.M. (Ed.), Metallization Associated with Acid Magmatism, vol. 6. John Wiley and Sons, Ltd., pp. 279–289.

Saupe, F., 1973. La Geologie du gisement de mercure d'Almadén province de Ciudad Real Espagne. B.R.G.M., Sciences de la Terre 29, 1–342.

Simpson, P.R., Brown, G.C., Plant, J., Ostle, D., 1979. Uranium mineralization and granite magmatism in the British Isles. Philosophical Transactions Royal Society of London, Series A 291, 385–412.

Štemprok, M., 1978. Differentiation of some elements by ore-bearing granites. In: Štemprok, M., Burnol, L., Voldán, J. (Eds.), Metallization Associated with Acid Magmatism, vol. 3. Geological Survey, Prague, pp. 393–403.

Stone, M., 1982. The behaviour of tin and some other trace elements during granite differentiation, West Cornwall, England. In: Evans, A.M. (Ed.), Metallization Associated with Acid Magmatism, vol. 6. John Wiley and Sons, Ltd., pp. 339–355.

Tamain, G., 1967. El Centenillo zone de reference pour l'etude de l'Ordovicien de la Sierra Morena Orientale Espagne. Comptes Rendus de l'Academie des Sciences, Paris 265, 389–392.

Tamain, G., 1972. Recherches Geologiques et minières en Sierra Morena Orientale, Espagne. PhD thesis 3eme cycle. Universite de Paris Sud. Centre d'Orsay, France. 870 pp.

Viets, J.G., Hopkins, R.T., Miller, B.M., 1992. Variations in minor and trace metals in sphalerite from Mississippi Valley-Type deposits of the Ozark Region: genetic implications. Economic Geology 87, 1897–1905.

Wagner, R.H., 1983. The Stephanian B of Puertollano. In: Quesada, C., Garrote, A. (Eds.), "Guidebook of field trip D: The Carboniferous of Sierra Morena". 10th International Carboniferous Congress, Madrid, pp. 16–22.

Wallis, R.L., 1985. Early evolution and sedimentation in the Puertollano basin (Ciudad Real, Central Spain). In: Lemos de Sousa, M.J., Wagner, R.H. (Eds.), Papers on the Carboniferous of the Iberian Peninsula Sedimentology, Paleontology, Tectonics and Geochronology, Annales Facultad de Ciências, Porto, vol. 64, pp. 269–282 (suppl).